

Three dimensional branching pipe flows for optimal scalar transport between walls

Anuj Kumar*

Abstract

We consider the problem of “wall-to-wall optimal transport” in which we attempt to maximize the transport of a passive temperature field between hot and cold plates. Specifically, we optimize the choice of the divergence-free velocity field in the advection-diffusion equation subject to an enstrophy constraint (which can be understood as a constraint on the power required to generate the flow). Previous work established an a priori upper bound on the transport, scaling as the $1/3$ -power of the flow’s enstrophy. Recently, Tobiasco & Doering (*Phys. Rev. Lett.* vol.118, 2017, p.264502) and Doering & Tobiasco (*Comm. Pure Appl. Math.* vol.72, 2019, p.2385–2448) constructed self-similar two-dimensional steady branching flows saturating this bound up to a logarithmic correction. This logarithmic correction appears to arise due to a topological obstruction inherent to two-dimensional steady branching flows. We present a construction of three-dimensional “branching pipe flows” that eliminates the possibility of this logarithmic correction and therefore identifies the optimal scaling as a clean $1/3$ -power law. Our flows resemble previous numerical studies of the three-dimensional wall-to-wall problem by Motoki, Kawahara & Shimizu (*J. Fluid Mech.* vol.851, 2018, p.R4). We also discuss the implications of our result to the heat transfer problem in Rayleigh–Bénard convection and the problem of anomalous dissipation in a passive scalar.

Contents

1	Introduction	2
1.1	Motivation	2
1.2	Problem setup	3
1.2.1	Steady case	4
1.2.2	Unsteady case	4
1.3	Previous work and the present results	5
1.4	Overview and philosophy of the proof	6
1.4.1	The variational principle	6
1.4.2	Convection rolls	7
1.4.3	Two-dimensional steady branching flows	8
1.4.4	Three-dimensional steady branching pipe flows	9
1.5	Organization of the paper	11
2	Notation and preliminaries	12
3	Step III of the construction: Proof of Theorem 1.1	13
4	Construction of three-dimensional branching pipe flow: Step I and Step II	15
4.1	A detailed sketch of the construction	15
4.2	Step I: Construction of the parent copies	16
4.2.1	The flow field $\bar{\mathbf{u}}$ and $\bar{\mathbf{u}}_b$	17
4.2.1.1	Patching up $\bar{\mathbf{u}}_1$ and $\bar{\mathbf{u}}_2$: Construction in the reducer region	20

*Department of Applied Mathematics, University of California Santa Cruz, CA 95064. Email: akumar43@ucsc.edu.

4.2.2	The scalar fields $\bar{\xi}$ and $\bar{\xi}_b$	22
4.3	Main copies $\bar{\mathbf{u}}_N$ and $\bar{\xi}_N$: Proof of Proposition 3.1	25
5	A useful estimate for the solution of the Poisson's equation: Proof of Proposition 3.2	30
5.1	Proof of Proposition 5.2	33
6	Discussion	38
6.1	Anomalous dissipation in a passive scalar	38
6.2	Rayleigh–Bénard convection	39
A	Derivation of the variational principle for heat transfer (1.11)	40
B	Bounds on a few integrals	42
C	A few basic lemmas	43

1 Introduction

1.1 Motivation

An important subdiscipline of thermal engineering is devoted to the design of heat exchangers, ventilation systems, air-conditioning systems, refrigeration systems, boilers, and chemical reactors [Aro00, Jak08, Thu13, AK18]. A fundamental challenge in this field is how to transport heat from a hot surface to a cold surface by moving the fluid using actuators such as fans or pumps, which can advect heat at a quicker rate than pure conduction. For most practical purposes, one would of course like to do so in the most economical way, minimizing the power supplied to the actuators. In the design of the systems described above, we would therefore like to know the answers to the following questions:

- (A) What is the optimal heat transfer rate as a function of the power supplied?
- (B) What is the corresponding placement of fans/pumps which maximizes the heat transfer for a given amount of power supplied?

To model the problem mathematically, we use the forced Navier–Stokes equation to describe the flow of an incompressible fluid:

$$\partial_t \mathbf{u} + \mathbf{u} \cdot \nabla \mathbf{u} = -\nabla p + \nu \Delta \mathbf{u} + \mathbf{f} \quad \text{in } \Omega,$$

where Ω is a bounded domain with smooth boundaries and ν is the viscosity of the fluid. We assume that the fluid satisfies a no-slip boundary condition on the surface, i.e., $\mathbf{u}|_{\partial\Omega} = \mathbf{0}$. In this mathematical formulation of the problem, the question of interest now involves finding the optimal design for the force \mathbf{f} that maximizes the heat transfer with a restricted mean power supply \mathcal{P}^* . Denoting the volume average and the long-time volume average, respectively, as

$$\oint_{\Omega} [\cdot] \, d\mathbf{x} = \frac{1}{|\Omega|} \int_{\Omega} [\cdot] \, d\mathbf{x} \quad \text{and} \quad \langle [\cdot] \rangle = \limsup_{\tau \rightarrow \infty} \frac{1}{\tau} \int_0^{\tau} \oint_{\Omega} [\cdot] \, d\mathbf{x} dt,$$

we can express the constraint on the mean power supply as $\langle \mathbf{f} \cdot \mathbf{u} \rangle \leq \mathcal{P}^*$.

Assuming the velocity field stays smooth and the kinetic energy of flow stays bounded in time, then the long-time spatial average of the energy equation leads to

$$\langle \mathbf{f} \cdot \mathbf{u} \rangle = \nu \langle |\nabla \mathbf{u}|^2 \rangle.$$

Physically, this means that the work done by the force \mathbf{f} to move the fluid is eventually dissipated viscously. It also shows that instead fixing the power supply, one can equivalently impose a constraint on the enstrophy of the flow, i.e., $\langle |\nabla \mathbf{u}|^2 \rangle \leq \nu^{-1} \mathcal{P}^*$.

The advantage of formulating the constraint in terms of the enstrophy is that we can from here on ignore the momentum equation entirely. We can simply ask, what is the flow \mathbf{u} that maximizes the heat transfer, for a given bound on the enstrophy ($\langle |\nabla \mathbf{u}|^2 \rangle \leq \nu^{-1} \mathcal{P}^*$). Once that flow \mathbf{u} is found, the corresponding forcing \mathbf{f} can then be computed from (1.1). Whether the optimal flow \mathbf{u} obtained in this manner is dynamically stable is a separate question that we will not address in this paper.

Beyond the primary engineering motivation, the optimal heat transport problem considered in this paper is also inspired by two problems: (1) anomalous dissipation in a passive scalar, (2) Rayleigh–Bénard convection. These problems, and their relationship with the optimal transport problem investigated here, will be discussed in section 6.

1.2 Problem setup

Although the problem discussed above is very general, we now focus on a special case in the simplest possible geometry namely the transport of a passive scalar T (which we refer to as temperature) by a flow field \mathbf{u} between two parallel walls held at different constant values of T . We assume that the flow field \mathbf{u} is incompressible and satisfies no-slip boundary conditions at the walls, which in the wall-normal coordinates are located at $z = -H/2$ and $z = H/2$, where H denotes the distance between the walls. The temperature field evolves according to the advection-diffusion equation

$$\partial_t T + \mathbf{u} \cdot \nabla T - \kappa \Delta T = 0, \quad (1.1)$$

and satisfies Dirichlet boundary conditions

$$T = T_B \text{ at } z = -H/2, \quad T = T_T \text{ at } z = H/2. \quad (1.2)$$

In (1.1), κ is the thermal diffusivity, and without loss of generality, we choose $T_B > T_T$ in (1.2). For simplicity, we consider the horizontal directions x and y to be periodic with length l_x and l_y . The domain of interest is thus given by $\Omega := \mathbb{T}_{l_x} \times \mathbb{T}_{l_y} \times (-H/2, H/2)$.

For a given flow field \mathbf{u} , we define the corresponding rate of heat transfer as

$$Q(\mathbf{u}) := \left\langle u_z T - \kappa \frac{\partial T}{\partial z} \right\rangle = \langle u_z T \rangle + \frac{\kappa(T_B - T_T)}{H}.$$

By performing the long-time horizontal average of equation (1.1), one can show that $Q(\mathbf{u})$ is equal to the heat flux at the top or the bottom boundary, hence the definition. Furthermore, by multiplying (1.1) with T and performing the long-time volume average, one can alternatively express the rate of heat transfer $Q(\mathbf{u})$ as

$$Q(\mathbf{u}) = \frac{\kappa H}{T_B - T_T} \langle |\nabla T|^2 \rangle.$$

The question of optimal heat transport described in the previous subsection seeks to find the maximum possible value of the heat transfer over all incompressible flow fields satisfying the no-slip boundary condition and the enstrophy constraint:

$$Q_{\max}(\mathcal{P}^*) := \sup_{\substack{\mathbf{u}(t, \mathbf{x}) \\ \nabla \cdot \mathbf{u} = 0, \mathbf{u}|_{\partial\Omega} = \mathbf{0} \\ \langle |\nabla \mathbf{u}|^2 \rangle \leq \nu^{-1} \mathcal{P}^*}} Q(\mathbf{u}).$$

Before we proceed further, we nondimensionalize the problem by making the following transformations, respectively, for the position, time, velocity field, temperature and the heat transfer:

$$\mathbf{x} \rightarrow H\mathbf{x}, \quad t \rightarrow \frac{H^2}{\kappa}t, \quad \mathbf{u} \rightarrow \frac{\kappa}{H}\mathbf{u}, \quad T \rightarrow (T_B - T_T)T + T_T, \quad Q \rightarrow \frac{\kappa(T_B - T_T)}{H}Q. \quad (1.3)$$

We continue to denote the nondimensional horizontal periodic lengths with l_x and l_y . After the rescaling (1.3),

a single nondimensional parameter remains, namely the nondimensional power given by

$$\mathcal{P} = \mathcal{P}^* \frac{H^4}{\nu \kappa^2}$$

which can be increased by either increasing the dimensional power supply \mathcal{P}^* and the domain size H or by decreasing the thermal diffusivity κ and viscosity ν of the fluid. After the nondimensionalization the enstrophy constraint becomes $\langle |\nabla \mathbf{u}|^2 \rangle \leq \mathcal{P}$.

As the problem of optimal heat transport can be considered both in two and three dimensions, let us define

$$\Omega^{2D} := \mathbb{T}_{l_x} \times (-1/2, 1/2), \quad \Omega^{3D} := \mathbb{T}_{l_x} \times \mathbb{T}_{l_y} \times (-1/2, 1/2). \quad (1.4a-b)$$

In the introduction, Ω is used to mean either Ω^{2D} or Ω^{3D} except in places where the distinction is required, in which case we will make the reference explicit. In rest of the paper Ω will only mean Ω^{3D} . Without the loss of generality, we assume that the aspect ratio of the domain satisfies $l_x \leq l_y$. Next, we explicitly formulate the steady, followed by the unsteady version of the optimal heat transport problem.

1.2.1 Steady case

In the steady case, we seek

$$Q_{\max}^s(\mathcal{P}) = \sup_{\substack{\mathbf{u} \in L^\infty(\Omega) \\ \nabla \cdot \mathbf{u} = 0, \mathbf{u}|_{\partial\Omega} = \mathbf{0} \\ \int_{\Omega} |\nabla \mathbf{u}|^2 d\mathbf{x} \leq \mathcal{P}}} Q(\mathbf{u}) \quad \text{where} \quad Q(\mathbf{u}) = \int_{\Omega} |\nabla T|^2 d\mathbf{x}, \quad (1.5)$$

and T solves the steady advection-diffusion equation with Dirichlet boundary conditions

$$\left. \begin{aligned} \mathbf{u} \cdot \nabla T - \Delta T &= 0, \\ T &= 1 \text{ at } z = -1/2, \quad T = 0 \text{ at } z = 1/2. \end{aligned} \right\} \quad (1.6)$$

1.2.2 Unsteady case

In the unsteady case, we seek

$$Q_{\max}^u(\mathcal{P}) = \sup_{\substack{\mathbf{u} \in L^\infty([0, \infty) \times \Omega) \\ \nabla \cdot \mathbf{u} = 0, \mathbf{u}|_{\partial\Omega} = \mathbf{0} \\ \langle |\nabla \mathbf{u}|^2 \rangle \leq \mathcal{P}}} Q(\mathbf{u}) \quad \text{where} \quad Q(\mathbf{u}) = \langle |\nabla T|^2 \rangle, \quad (1.7)$$

and T solves the unsteady advection-diffusion equation with Dirichlet boundary conditions

$$\left. \begin{aligned} \partial_t T + \mathbf{u} \cdot \nabla T - \Delta T &= 0, \\ T &= T_0 \in L^2(\Omega) \text{ at } t = 0, \\ T &= 1 \text{ at } z = -1/2, \quad T = 0 \text{ at } z = 1/2 \quad \forall t \in (0, \infty). \end{aligned} \right\} \quad (1.8)$$

Remark 1.1. It is clear that for every \mathcal{P} , we have the inequality $Q_{\max}^s \leq Q_{\max}^u$. Therefore, any upper bound on Q_{\max}^u provides an upper bound on Q_{\max}^s . Similarly, any lower bound on Q_{\max}^s is a lower bound on Q_{\max}^u as well.

Remark 1.2. The values of Q_{\max}^s and Q_{\max}^u for the three-dimensional problem are larger than their corresponding values for the two-dimensional problem. This is because any two-dimensional solution of the advection diffusion equation is also a solution in three-dimensions by an extension that is invariant in the third direction.

Remark 1.3. In the unsteady case, the quantity $Q(\mathbf{u})$ does not depend on the initial condition T_0 as long as this initial condition belongs to $L^2(\Omega)$. Physically, this means that the dependence of the solution T on the initial data is lost at long times because of the presence of diffusion.

For both the steady and unsteady cases, in their two- and three-dimensional versions, the questions of prime importance are:

- (A) How the maximum heat fluxes Q_{\max}^s and Q_{\max}^u scale as a function of the input power \mathcal{P} for asymptotically large values of \mathcal{P} ?
- (B) What does the structure of the flow fields that transfer heat “most efficiently” look like?

In this paper, we investigate these questions for the steady case only. The unsteady case is also of great importance and will be considered in a future study.

1.3 Previous work and the present results

The problem of optimal heat transport between parallel walls, as described above, was first introduced in the work of Hassanzadeh, Chini and Doering [HCD14] whose motivation was to improve previously known upper bounds on heat transfer in porous medium convection [DC98] and Rayleigh–Bénard convection [DC96, PK03, WD11, WCKD15]. Using numerical and matched asymptotic techniques, they studied the problem in two dimensions, applying either the energy or enstrophy constraints on the velocity field which satisfies stress-free boundary conditions.

Their initial investigation has since inspired several studies of optimal heat transport between differentially heated plates [TD17, MKS18, DT19, STD20] and slightly different problem of optimal cooling of a fluid subjected to a given volumetric heating [MDTY18, IV22, Tob21]. Of all these studies, the three of particular interest to the current paper are [TD17], [MKS18] and [DT19]. They all investigate the same problem considered in this paper, i.e., optimal heat transport between parallel boundaries by incompressible flows satisfying no-slip boundary conditions with an enstrophy constraint. Doering & Tobasco ([DT19]) derived an upper bound on the maximum possible heat transfer, and showed that any flow satisfying the required constraint cannot transport heat faster than a rate proportional to the enstrophy to the power of $1/3$, i.e.,

$$Q_{\max}^u(\mathcal{P}) \leq C' \mathcal{P}^{1/3} \quad \text{for } \mathcal{P} \geq C'', \quad (1.9)$$

where C' is a universal constant but C'' depends on the aspect ratio. This upper bound is valid both in two and three dimensions and applies to $Q_{\max}^s(\mathcal{P})$ as well (see Remark 1.1). The same bound had been proved before in the context of Rayleigh–Bénard convection in at least three different ways: using the variational principle of Howard ([How63, Bus69]), the background method of Doering & Constantin ([DC96, PK03]) and more recently by Seis ([Sei15]).

Complimentary to their upper bound, [TD17] and [DT19] constructed two-dimensional steady branching flows (in which the flow structures have increasingly fine scales as one approaches the boundary, see figure 2b) and showed that the upper bound could be attained up to an unknown logarithmic correction. More specifically, they showed

$$\frac{\mathcal{P}^{1/3}}{\log^{4/3} \mathcal{P}} \lesssim Q_{\max}^s(\mathcal{P}).$$

Soon after the work of [TD17], Motoki, Kawahara and Shimizu [MKS18], through a numerical optimization procedure, discovered complicated but rather beautiful three-dimensional steady branching flows (depending on \mathcal{P}) that appears to display a heat transfer rate $Q_{\max}^s(\mathcal{P}) \sim \mathcal{P}^{1/3}$.

In this paper, we rigorously show that $\mathcal{P}^{1/3} \lesssim Q_{\max}^s(\mathcal{P})$ by constructing three-dimensional steady branching pipe flows. Our main result is:

Theorem 1.1 (Steady three-dimensional case). *Let Ω be Ω^{3D} as defined in (1.4a-b). Then there exists two positive constants \mathcal{P}_0 and C such that Q_{\max}^s , as defined in (1.5), obeys the following lower bound:*

$$C \mathcal{P}^{1/3} \leq Q_{\max}^s(\mathcal{P})$$

for $\mathcal{P}_0 \leq \mathcal{P}$. The constants \mathcal{P}_0 and C depends on l_x as follows:

$$\mathcal{P}_0(l_x) = \frac{1 + l_x^2}{l_x^2} \mathcal{P}'_0, \quad C(l_x) = \frac{l_x^{8/3}}{1 + l_x^{8/3}} C',$$

where $\mathcal{P}'_0, C' > 0$ are two universal constants.

Remark 1.4. Combining the result of Theorem 1.1 with upper bound (1.9) and Remark 1.1, we fully characterize the exact behavior of maximum heat transfer in three dimensions. In particular, we have $Q_{\max}^s \sim \mathcal{P}^{1/3}$ (as a result $Q_{\max}^u \sim \mathcal{P}^{1/3}$) in three dimensions. Whether $Q_{\max}^s \sim \mathcal{P}^{1/3}$ in two dimensions as well is an open problem (see Conjecture 1.3).

Remark 1.5. It clear that if $l_x \geq 1$ then \mathcal{P}_0 and C are bounded from below by two positive constants independent of l_x . Therefore, assuming $l_x \geq 1$, i.e., for sufficiently wide domains, we can also restate the above theorem where \mathcal{P}_0 and C are two positive constants independent of any parameter.

Remark 1.6. We consider here a periodic setting in the x and y directions. As the flows that we construct to prove the theorem have a compact support in space, the theorem remains true if Ω is a closed box of size l_x and l_y with insulating and no-slip side walls.

1.4 Overview and philosophy of the proof

1.4.1 The variational principle

The proof of Theorem 1.1 relies on a variational principle for the heat transfer derived by [DT19] which was inspired by the work in homogenization theory such as of [AM91, FP94] about estimating the effective diffusivity in a random or periodic array of vortices. To state the result, we start by defining two admissible sets:

$$\mathcal{A}^s := L^\infty(\Omega; \mathbb{R}^3) \cap H_0^1(\Omega; \mathbb{R}^3), \quad (1.10a)$$

$$\mathcal{X}^s := H_0^1(\Omega). \quad (1.10b)$$

For steady velocity fields, the variational principle associated with the maximization of heat transfer can be stated as

Proposition 1.2 ([DT19]). *For Q_{\max}^s given by (1.5), we have*

$$Q_{\max}^s(\mathcal{P}) - 1 = \sup_{\substack{\mathbf{u} \in \mathcal{A}^s \\ \nabla \cdot \mathbf{u} = 0}} \sup_{\substack{\xi \in \mathcal{X}^s \\ \xi \neq 0}} \frac{(\int_{\Omega} u_z \xi \, d\mathbf{x})^2}{\int_{\Omega} |\nabla \Delta^{-1}(\mathbf{u} \cdot \nabla \xi)|^2 \, d\mathbf{x} + \frac{1}{\mathcal{P}} \int_{\Omega} |\nabla \mathbf{u}|^2 \, d\mathbf{x} \int_{\Omega} |\nabla \xi|^2 \, d\mathbf{x}}. \quad (1.11)$$

In (1.11), Δ^{-1} denotes the inverse Laplacian operator in Ω corresponding to the homogeneous Dirichlet boundary conditions. For completeness, we provide a derivation of this variation principle in the Appendix A. The derivation is taken from ([DT19]).

From the variational principles (1.11), we see that any choice of admissible velocity field \mathbf{u} and scalar field ξ provides a lower bound on the heat transfer. Our goal, therefore, is to find a “good” flow field \mathbf{u} (depending on \mathcal{P}), and a corresponding ξ , for which the dependence on \mathcal{P} of the lower bound obtained matches that of the theoretical upper bound (1.9), namely, $\mathcal{P}^{1/3}$.

We closely analyze each term involved in the variational principle (1.11). We label them

$$I = \left(\int_{\Omega} u_z \xi \, d\mathbf{x} \right)^2, \quad II = \int_{\Omega} |\nabla \Delta^{-1}(\mathbf{u} \cdot \nabla \xi)|^2 \, d\mathbf{x}, \quad III = \frac{1}{\mathcal{P}} \int_{\Omega} |\nabla \mathbf{u}|^2 \, d\mathbf{x} \int_{\Omega} |\nabla \xi|^2 \, d\mathbf{x}, \quad (1.12a-c)$$

and identify them as the transport term (I), the nonlocal term (II) and the dissipation term (III), respectively.

In order to obtain a good lower bound, we would ideally like to choose \mathbf{u} and ξ to maximize the right-hand side of (1.11) as much as possible. This, in turn, means we should aim to maximize I and minimize II and III .



Figure 1: Panel (a) illustrates good and bad strategies to maximize term I defined in (1.12a-c). In the good scenario ξ is positive (indicated by red color) where the flow is moving upward (positive z -direction) and is negative (blue color) where the flow is moving downward. Therefore, u_z and ξ are positively correlated. This is not the case in the bad scenario. Panel (b) illustrates good and bad strategies to minimize term II . In the good scenario $\nabla\xi$ is perpendicular to \mathbf{u} , hence $\mathbf{u} \cdot \nabla\xi \equiv 0$, i.e., ξ is constant along the streamlines and therefore the term II is zero. In the bad scenario $\nabla\xi$ is parallel to \mathbf{u} , so the term II is nonzero.

To maximize I , we should choose a \mathbf{u} such that its z -component is “positively correlated” with the ξ field. Figure 1a shows examples of a good and bad scenario. To minimize II , we should make a choice such that \mathbf{u} is perpendicular to $\nabla\xi$ in most of the domain, which can alternatively be stated as ξ should be constant along the streamlines of the flow \mathbf{u} . Figure 1b shows examples of a good and bad scenario.

Our aim at this point is to provide heuristic but compelling arguments why trial velocity profiles such as (i) standard convection rolls and (ii) the two-dimensional steady branching flows considered by [TD17, DT19] are not sufficient to prove Theorem 1.1. By diligently inspecting the limitations of these trial flow fields, we are then naturally led to propose three-dimensional branching pipe flows as a remedy.

1.4.2 Convection rolls

The first choice of a trial velocity profile \mathbf{u} that comes to mind is the one associated with planar convection rolls, as this is one of the simplest incompressible flow fields capable of transporting heat by advection. Figure 2a shows the streamlines of typical convection rolls. In the bulk region, far from the horizontal walls, the flow either moves up or down. To maintain the incompressibility constraint, the flow must turn around in a boundary layer near the walls. We then select a ξ field accordingly, in an attempt to maximize I and minimize II (see figure 1).

The advantage of this configuration is that it is possible to restrict the region where $\mathbf{u} \cdot \nabla\xi$ is non-zero (which eventually contributes toward II) to the boundary layer only. However, this choice turns out to be particularly bad with respect to term III . Indeed, assuming the flow velocity $\mathbf{u} \sim 1$ in the bulk region, then we must have a “large” fluid velocity $\mathbf{u} \sim \ell/\delta$ in the boundary layer because of the incompressibility condition, where ℓ is the aspect ratio of a single convection roll. Consequently, $\nabla\mathbf{u} \sim \ell/\delta^2$, which essentially becomes “very large” for small boundary layer thickness δ . Performing a formal scaling analysis of each individual terms in the variational principle (1.11) leads to

$$Q_{\max}^s \gtrsim \frac{1}{\delta + \frac{1}{\mathcal{P}} \left(\frac{\ell^2}{\delta^4} + \frac{1}{\ell^4} \right)}.$$

The right-hand side is optimized by choosing $\delta \sim \mathcal{P}^{-3/11}$ and $\ell \sim \mathcal{P}^{-2/11}$, which leads to

$$Q_{\max}^s \gtrsim \mathcal{P}^{3/11}.$$

This scaling recovers the result of [STD20], who rigorously showed that $Q^s(\mathbf{u}) \sim \mathcal{P}^{3/11}$ for a particular choice of convective rolls, as well as the results of [How63, DC96] who found the same scaling in the context of Rayleigh–Bénard convection. The exponent $3/11$ is clearly less than $1/3$ suggesting that the convection rolls may not be the most efficient way of transporting heat at high \mathcal{P} .

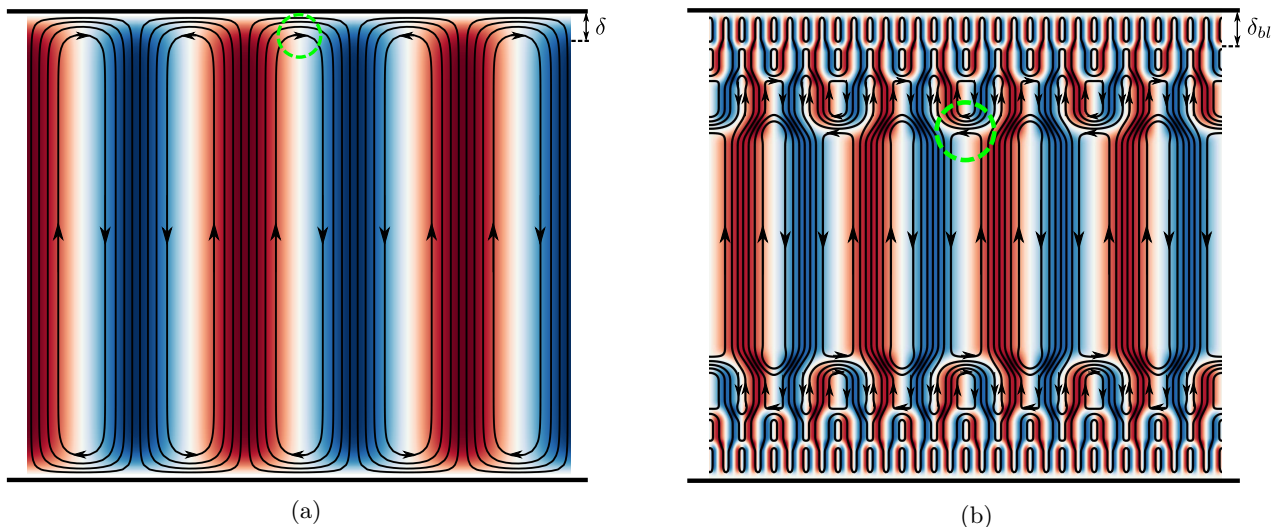


Figure 2: Panel (a) shows the streamlines of a set of typical convective rolls. Panel (b) shows the streamlines of a steady two dimensional branching flow. In both figures, the streamlines have been overlayed with a ξ field according to the good scenario described in figure 1a (i.e. ξ is positive whenever u_z is positive, and ξ is negative whenever u_z is negative). The red color indicates a positive value of ξ , whereas the blue color indicates a negative value. The dashed circles in both the figures show a region where $\mathbf{u} \cdot \nabla \xi$ is nonzero.

1.4.3 Two-dimensional steady branching flows

One way to improve the heat transport is to consider a flow field with a branching structure, i.e., where the scale of flow structures becomes smaller (possibly in a self-similar manner) as one approaches the walls, an idea that goes back to Busse ([Bus69]). The branching ends after a finite number of steps, which depends on \mathcal{P} . The idea behind the branching is to continue dividing the flow into “multiple channels” as it moves towards the wall, which helps maintain the typical magnitude of the velocity field to be order unity throughout the domain. Assuming δ_{bl} is the vertical thickness of the last branching level (namely, the boundary layer), then for the branching flows we have $\nabla \mathbf{u} \sim \delta_{bl}^{-1}$ in the boundary layer, which is significantly smaller than $\nabla \mathbf{u} \sim \delta_{bl}^{-2}$ in the case of convection rolls.

A replica of the two-dimensional steady branching flow structure constructed by [TD17, DT19] is shown in figure 2b and we have overlaid the streamlines with a ξ field according to the good scenario shown in figure 1a. Branching in two dimensions requires some part of the flow to fold back at every branching level. Although this solves the problem regarding the term III , it creates a different topological issue. From figure 2b it becomes clear that $\nabla \xi$ is parallel to \mathbf{u} not just in the boundary layer but also in the bulk at every branching level. A typical region is shown in dashed circle in figure 2b. The result is that $\mathbf{u} \cdot \nabla \xi$ is nonzero (which ultimately contributes towards the term II) in a significant portion of the domain compared with the case of convection rolls where this term was nonzero only in the boundary layer. Furthermore, there does not appear to be a way around this topological obstruction by simply choosing a different ξ field. This is because the streamlines of the flow \mathbf{u} continually fold back throughout the branching structure, from the bulk to the boundary layer, (see figure 2b) and leaving only very few streamlines to continue towards the boundary layer. So it appears that if we follow the good strategy in figure 1a (which is to choose ξ positive where u_z is positive and vice-versa) then it is impossible to maintain ξ constant along streamlines (even in the bulk), hence we pay towards term II . If we avoid the good strategy in figure 1a, then it is not possible to make the term I “large.” However, it turns out the situation is still much better than the convection rolls and a formal scaling analysis (see [DT19]) shows

$$Q_{\max}^s \gtrsim \frac{1}{\ell_{bl} + \int_{\frac{1}{2}}^{1-\delta_{bl}} (\ell')^2 dz + \frac{1}{\mathcal{P}} \left(\frac{1}{\ell_{bulk}^2} + \int_{\frac{1}{2}}^{1-\delta_{bl}} \frac{1}{\ell'^2} dz + \frac{1}{\ell_{bl}} \right)^2},$$

where ℓ_{bulk} and ℓ_{bl} denotes the horizontal aspect ratio of a typical roll in the bulk region and in the boundary layer region, respectively, while the function $\ell(z)$ denotes how the aspect ratio changes as a function of the z coordinate. After optimizing the unknown parameters ($\delta_{bl}, l_{bulk}, l_{bl}$ and $l(z)$), one can only show

$$Q_{\max}^s \gtrsim \frac{\mathcal{P}^{1/3}}{\log^{4/3} \mathcal{P}},$$

which is result of [TD17, DC96]

Whether there exists a two-dimensional steady flow that can overcome the topological obstruction elaborated above to show $\mathcal{P}^{1/3} \lesssim Q_{\max}^s$ is an open question. Based on the heuristic reasons given previously, we believe that there are no such flows and therefore conjecture the following.

Conjecture 1.3 (Weak). *Let Ω be Ω^{2D} given by (1.4a-b). Then the heat transfer defined in (1.5) obeys*

$$Q_{\max}^s = o(\mathcal{P}^{1/3})$$

for large \mathcal{P} , where ‘ o ’ denotes the little- o .

The weak conjecture states that Q_{\max}^s is asymptotically smaller than $\mathcal{P}^{1/3}$ but does not identify the correct asymptotic scaling of Q_{\max}^s at large \mathcal{P} . It is reasonable to assume that the lower bound estimate of [TD17, DT19] could be sharp. We therefore conjecture:

Conjecture 1.4 (Strong). *Let Ω be Ω^{2D} given by (1.4a-b). Then the heat transfer defined in (1.5) obeys*

$$Q_{\max}^s \sim \frac{\mathcal{P}^{1/3}}{\log^{4/3} \mathcal{P}},$$

for large \mathcal{P} .

We strongly believe that the weak conjecture is true but not so much that the strong conjecture is also true.

1.4.4 Three-dimensional steady branching pipe flows

The novelty of this work comes from the realization that the topological obstruction discussed above, can be overcome by taking advantage of the third dimension. Indeed, in three dimensions, it is possible to construct flow channels with a branching structure that continues all the way to the wall without the need for the flow to fold back as in the two-dimensional case. Therefore, in three dimensions, it is possible to construct a flow field \mathbf{u} and a scalar field ξ that have a branching structure while maintaining $\mathbf{u} \cdot \nabla \xi = 0$ everywhere except in the boundary layer (which overcomes the difficulty faced in two-dimensional steady branching flows). The construction in this paper is self-similar and the resultant flow field \mathbf{u} looks like branching pipe flow. The parent construct used in the self-similar construction is shown in figure 3a. It consists of two different type of pipes, one in which the flow moves up (shown in red, we choose ξ positive in this region) and one in which the flow moves down (shown in blue, we choose ξ negative in this region). By placing appropriately scaled copies of this parent construct along the tree structure shown in figure 3b, we obtain the desired flow field. The self-similar construction does not continue forever but truncates after a finite number of levels depending on the value of \mathcal{P} . After a fixed number of levels, the flow finally folds back in the boundary layer, according to the construct shown in figure 3c. This is the region where the hot and cold pipelines finally merge and $\mathbf{u} \cdot \nabla \xi$ is nonzero. A two-dimensional cartoon of this three-dimensional branching pipe structure is shown in figure 4. This cartoon also emphasizes the topological obstruction in two dimensions which informally can be expressed as “it is not possible to build two branching channels, one hot (in which the flow moves up) and other one cold (in which the flow moves down), in two-dimensions without having them intersect.”

Using this branching pipe flow a formal scaling analysis of the heat transfer yields

$$Q_{\max}^s \gtrsim \frac{1}{2^{-N} + \frac{4^N}{\mathcal{P}}},$$

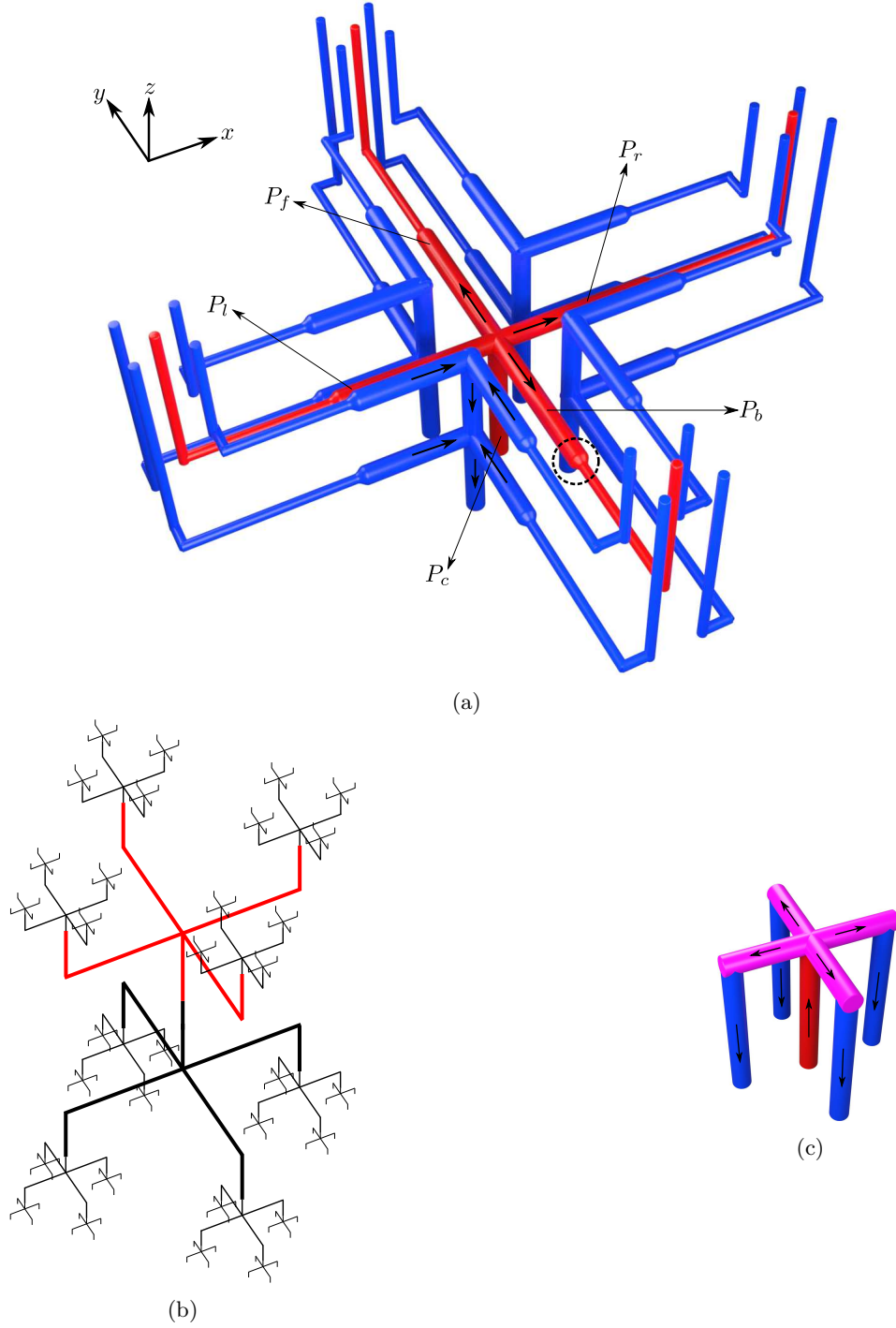


Figure 3: Illustration of the branching pipe flow. Panel (a): the parent construct $\bar{\mathbf{u}}$. It consists of red and blue pipes which are the part of pipelines \mathbf{P}_{up} and \mathbf{P}_{down} , respectively. In panel (a), arrows are used in some pipes to show the direction of the flow. The reducer region of a pipe is also shown using a dashed circle. Panel (b): the branching skeleton. To build the main copy $\bar{\mathbf{u}}_N$ away from the boundary layer, we place the appropriately dilated version of the parent construct $\bar{\mathbf{u}}$ along the skeleton up to N levels. Panel (c): the parent construct $\bar{\mathbf{u}}_b$, which we use in the boundary layer. In the construct $\bar{\mathbf{u}}_b$, the flow from red pipes turn back to blue pipes (shown in the pink color). A 2D cartoon of the resultant pipe flow is shown in figure 4.

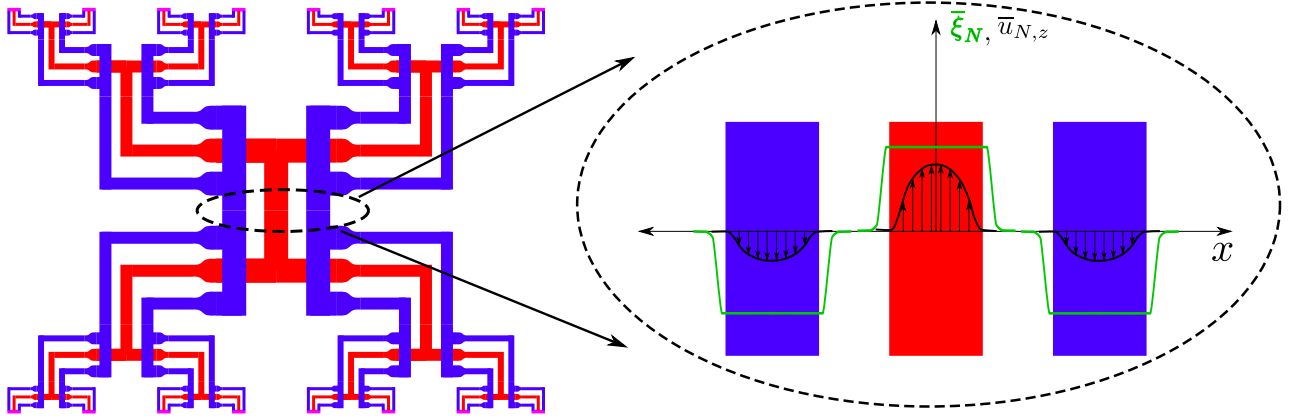


Figure 4: shows a 2D cartoon of the main copy $\bar{\mathbf{u}}_N$. The pipeline P_{up} is shown in red color and the pipeline P_{down} is shown in blue color. In the blow-up figure of a section of the pipeline, the graph of $\bar{\xi}_N$ is also shown. Notice is that $\bar{\xi}_N$ is constant in the support of $\bar{\mathbf{u}}_N$.

where N denotes the number of branching levels. After choosing $N = \lceil \log_2 \mathcal{P}^{1/3} \rceil$, we find that $Q_{\max}^s \gtrsim \mathcal{P}^{1/3}$. Theorem 1.1 is the rigorous result of this statement, which will be proved in the subsequent sections. The construction carried out in this paper can be summarized in three steps.

- Step I: Creating the parent constructs (the building blocks)
The velocity fields from this step form the basis for the self-similar construction in the second step. In this step, we construct (i) $\bar{\mathbf{u}}$ (figure 3a), which is used to build branching flow away from the boundary layer. (ii) $\bar{\mathbf{u}}_b$ (figure 3c), which is used in the boundary layer to truncate the branching structure.
- Step II: Construction of the main copy (a single tree)
In this step, we assemble the appropriately dilated copies of the parent constructs from the previous step to build the flow field $\bar{\mathbf{u}}_N$ (a 2D cartoon is shown in figure 4). Here, N denotes the number of branching levels which depends on \mathcal{P} . We also refer to this main copy as a single tree.
- Step III: Construction of the final flow field (a forest)
The flow field constructed in the last step is enough to capture the correct dependence of Q_{\max}^s on \mathcal{P} . However, to capture the correct dependence on the domain aspect ratio l_x and l_y , we build the final flow field \mathbf{u} by placing several copies of the tree side-by-side to fill the whole domain, which then looks like a forest.

1.5 Organization of the paper

The rest of paper is organized as follows. In section 2, we introduce a few notations and preliminaries that will be frequently used throughout the paper. In section 3, we perform Step III of the construction and prove the main theorem. We provide a detailed sketch of the parent constructs in section 4. We then carry out Step I and Step II. We provide a proof of Proposition 3.2 (essential for the analysis of the nonlocal term defined in (1.12a-c)) in section 5. We close by discussing implications of our results in section 6. A few of the more cumbersome but trivial calculations required to finish the proofs are carried out in appendices.

Acknowledgement

A.K. thanks P. Garaud for a careful read of the paper and providing comments. A.K. also thanks I. Tobasco

for providing comments, an invitation to visit University of Illinois Chicago and for several useful discussions.

2 Notation and preliminaries

The three domains we will be frequently using in this paper are: \mathbb{R}^3 , Ω and D , where

$$\Omega := \mathbb{T}_{l_x} \times \mathbb{T}_{l_y} \times (-1/2, 1/2), \quad D := \mathbb{R}^2 \times (-1/2, 1/2). \quad (2.1a-b)$$

Here, for some $l > 0$, $\mathbb{T}_l := (\mathbb{R}/l\mathbb{Z})$ and \mathbb{T}_l is identified with $[-l/2, l/2)$ in the usual way. In the rest of this section, V will denote either of these three domains: \mathbb{R}^3 , Ω and D , whereas \tilde{V} will denote either \mathbb{R}^3 or D . Let $\mathbf{x}, \mathbf{x}' \in \tilde{V}$, for which we denote

$$\mathbf{x}_{\parallel} := (x, y, 0), \quad \text{and} \quad |\mathbf{x} - \mathbf{x}'|_{\parallel} := |\mathbf{x}_{\parallel} - \mathbf{x}'_{\parallel}|, \quad (2.2a-b)$$

where $|\cdot|$ denotes the Euclidean distance. Let $S \subseteq V$, we will use $\mathbf{1}_S$ to denote the indicator function corresponding to the set S .

We define the support of a scalar or a vector-valued function f on V as

$$\text{supp } f := \overline{\{\mathbf{x} \in V \mid f(\mathbf{x}) \neq 0\}}, \quad (2.3)$$

and the support only in the z variable as

$$\text{supp}_z f := \overline{\{z \in \mathbb{R} \mid (x, y, z) \in V, f(x, y, z) \neq 0\}}. \quad (2.4)$$

For a given $\mathbf{p} \in \mathbb{R}^3$, we define a translation map $T^{\mathbf{p}} : \mathbb{R}^3 \rightarrow \mathbb{R}^3$ as $T^{\mathbf{p}}(\mathbf{x}) = \mathbf{x} + \mathbf{p}$. The inverse map is therefore denoted as $T^{-\mathbf{p}}$. Then, if f is a scalar function or a vector-valued function on \mathbb{R}^3 , we define the corresponding translated function $T^{\mathbf{p}}f$ as

$$(T^{\mathbf{p}}f)(\mathbf{x}) = f(T^{-\mathbf{p}}(\mathbf{x})), \quad \text{where } \mathbf{x} \in \mathbb{R}^3. \quad (2.5)$$

Similarly, for a given $\theta \in [0, 2\pi]$, we define a rotation map $\rho_{\theta} : \tilde{V} \rightarrow \tilde{V}$, which performs a counterclockwise rotation in the xy -plane by an angle θ . We denote the inverse map by $\rho_{-\theta}$. Then, if ζ is a scalar function on \tilde{V} , we define the corresponding rotated scalar function $\rho_{\theta}\zeta$ on \tilde{V} as

$$(\rho_{\theta}\zeta)(\mathbf{x}) = \zeta(\rho_{-\theta}(\mathbf{x})), \quad \text{where } \mathbf{x} \in \tilde{V}. \quad (2.6)$$

Furthermore, if \mathbf{v} is a vector-valued function defined on \tilde{V} , we define the corresponding rotated vector-valued function $\rho_{\theta}\mathbf{v}$ on \tilde{V} as

$$(\rho_{\theta}\mathbf{v})(\mathbf{x}) = \rho_{\theta}(\mathbf{v}(\rho_{-\theta}(\mathbf{x}))), \quad \text{where } \mathbf{x} \in \tilde{V}. \quad (2.7)$$

Let's denote the σ -algebra of Borel sets by $\mathcal{B}(\mathbb{R}^3)$. Given a Radon measure $\mu : \mathcal{B}(\mathbb{R}^3) \rightarrow \mathbb{R}$ and a vector field $\mathbf{u} \in L^1_{loc}(\mathbb{R}^3; \mathbb{R}^3, \mu)$, the set function $\nu : \mathcal{B}(\mathbb{R}^3) \rightarrow \mathbb{R}^3$

$$\nu := (\nu_x, \nu_y, \nu_z) := (u_x\mu, u_y\mu, u_z\mu) \quad (2.8)$$

is called a vector-valued Radon measure. Alternate shorthand notation is $\nu = \mathbf{u}\mu$. The Riesz's theorem ensures that the space of vector-valued Radon measure \mathcal{M} is dual to the space of compactly supported continuous vector fields $C_c(\mathbb{R}^3; \mathbb{R}^3)$ [GMS98, Mag12].

Now given a function $f \in C_c(\mathbb{R}^3)$ and $\nu \in \mathcal{M}$ as defined in (2.8), the integration of f with respect to the measure ν is a vector in \mathbb{R}^3 and is given by

$$\int_{\mathbb{R}^3} f d\nu = \left(\int_{\mathbb{R}^3} f u_x d\mu, \int_{\mathbb{R}^3} f u_y d\mu, \int_{\mathbb{R}^3} f u_z d\mu \right), \quad (2.9)$$

and the convolution is given by

$$(f * \nu)(\mathbf{x}) = \int_{\mathbb{R}^3} f(\mathbf{x} - \mathbf{x}') d\nu(\mathbf{x}'). \quad (2.10)$$

3 Step III of the construction: Proof of Theorem 1.1

In this section we begin by performing Step III of the construction. We assume the existence of main copies $\bar{\mathbf{u}}_N$ and $\bar{\xi}_N$ with properties stated in the proposition below. Then we place several of these copies together in Ω , to build the flow field \mathbf{u} and scalar field ξ , which we then use in the variational principle (1.11) to prove Theorem 1.1.

Proposition 3.1. *For every positive integer N , there exist $\bar{\mathbf{u}}_N \in C_c^\infty(D; \mathbb{R}^3)$ and $\bar{\xi}_N \in C_c^\infty(D)$ such that*

- (i) $\nabla \cdot \bar{\mathbf{u}}_N \equiv 0$,
- (ii) $\text{supp } \bar{\mathbf{u}}_N \cup \text{supp } \bar{\xi}_N \subseteq (-1/2, 1/2) \times (-1/2, 1/2) \times (-1/2, 1/2)$,
- (iii) $\text{supp}_z(\bar{\mathbf{u}}_N \cdot \nabla \bar{\xi}_N) \subseteq (1/2 - c_1 2^{-N}, 1/2 - c_2 2^{-N}) \cup (-1/2 + c_2 2^{-N}, -1/2 + c_1 2^{-N})$,
- (iv) $\|\bar{\mathbf{u}}_N \cdot \nabla \bar{\xi}_N\|_{L^\infty(D)} \lesssim 2^N$,
- (v) $\int_D |\nabla \bar{\mathbf{u}}_N|^2 d\mathbf{x} + \int_D |\nabla \bar{\xi}_N|^2 d\mathbf{x} \lesssim 2^N$,
- (vi) $\int_D \bar{u}_{N,z} \bar{\xi}_N d\mathbf{x} \geq c_3 > 0$,

Here, $0 < c_2 < c_1 < 1$ and c_3 are constants independent of N and $\bar{u}_{N,z}$ is the z -component of $\bar{\mathbf{u}}_N$.

Proof of Theorem 1.1. We construct \mathbf{u} (and ξ) by appropriately placing the several horizontally scaled copies of $\bar{\mathbf{u}}_N$ (and $\bar{\xi}_N$) from Proposition 3.1 side-by-side (see below for details). Specifically, let n_x and n_y be two positive integers, then we place $n_x n_y$ copies of $\bar{\mathbf{u}}_N$ (and $\bar{\xi}_N$) in a two-dimensional rectangular horizontal array. Then from the conditions on $\bar{\mathbf{u}}_N$ and $\bar{\xi}_N$ given in Proposition 3.1, we obtain estimates on various terms in the expression (1.11) and show that the desired lower bound on Q_{\max}^s , stated in Theorem 1.1, can be obtained.

More specifically, given $n_x, n_y \in \mathbb{N}$, we define two lengths d_x and d_y as follows:

$$d_x = \frac{l_x}{n_x} \quad \text{and} \quad d_y = \frac{l_y}{n_y}.$$

Next, we define $\mathbf{u} : D \rightarrow \mathbb{R}^3$ and $\xi : D \rightarrow \mathbb{R}$ as

$$\begin{aligned} \mathbf{u} \left(x d_x - \frac{l_x}{2} + \frac{2i-1}{2} d_x, y d_y - \frac{l_y}{2} + \frac{2j-1}{2} d_y, z \right) &:= \bar{\mathbf{u}}_N(x, y, z) \\ \xi \left(x d_x - \frac{l_x}{2} + \frac{2i-1}{2} d_x, y d_y - \frac{l_y}{2} + \frac{2j-1}{2} d_y, z \right) &:= \bar{\xi}_N(x, y, z) \end{aligned}$$

for all $i, j \in \mathbb{Z}$ and $(x, y, z) \in (-1/2, 1/2) \times (-1/2, 1/2) \times (-1/2, 1/2)$, otherwise, $\mathbf{u} := \mathbf{0}$ and $\xi := 0$. It is clear that \mathbf{u} and ξ are $l_x - l_y$ -periodic functions. It is the identification of these $l_x - l_y$ -periodic functions with functions on $\Omega = \mathbb{T}_{l_x} \times \mathbb{T}_{l_y} \times (-1/2, 1/2)$, which we continue to denote as \mathbf{u} and ξ , that we use throughout.

By construction, $\mathbf{u} \in C_c^\infty(\Omega; \mathbb{R}^3)$ and $\xi \in C_c^\infty(\Omega)$ and therefore belongs to the admissible sets \mathcal{A}^s and \mathcal{X}^s as defined in (1.10a) and (1.10b), respectively. Now one can estimate important terms in the variational formula (1.11). Let's start with the following:

$$\begin{aligned} \int_\Omega |\nabla \mathbf{u}|^2 d\mathbf{x} &= \frac{1}{l_x l_y} \int_\Omega |\nabla \mathbf{u}|^2 d\mathbf{x} = \frac{n_x n_y}{l_x l_y} \int_{-\frac{l_x}{2}}^{-\frac{l_x}{2} + d_x} \int_{-\frac{l_y}{2}}^{-\frac{l_y}{2} + d_y} \int_{-\frac{1}{2}}^{\frac{1}{2}} |\nabla \mathbf{u}|^2 d\mathbf{x} \\ &\lesssim \frac{n_x n_y d_x d_y}{l_x l_y \min\{d_x^2, d_y^2, 1\}} \int_D |\nabla \bar{\mathbf{u}}_N|^2 d\mathbf{x} \lesssim \frac{n_x n_y d_x d_y}{l_x l_y \min\{d_x^2, d_y^2, 1\}} 2^N. \end{aligned} \quad (3.2)$$

Similarly, we have

$$\int_{\Omega} |\nabla \xi|^2 d\mathbf{x} \lesssim \frac{n_x n_y d_x d_y}{l_x l_y \min\{d_x^2, d_y^2, 1\}} \int_D |\nabla \bar{\xi}_N|^2 d\mathbf{x} \lesssim \frac{n_x n_y d_x d_y}{l_x l_y \min\{d_x^2, d_y^2, 1\}} 2^N. \quad (3.3)$$

In a same way, one can also show

$$\int_{\Omega} u_z \xi d\mathbf{x} = \frac{n_x n_y d_x d_y}{l_x l_y} \int_D \bar{u}_{N,z} \bar{\xi}_N d\mathbf{x} \geq \frac{n_x n_y d_x d_y c_3}{l_x l_y}, \quad (3.4)$$

Finally, we have

$$\|\mathbf{u} \cdot \nabla \xi\|_{L^\infty(\Omega)} \lesssim \frac{2^N}{\min\{d_x, d_y, 1\}}, \quad (3.5)$$

with

$$\text{supp}_z(\mathbf{u} \cdot \nabla \xi) \subseteq (1/2 - c_1 2^{-N}, 1/2 - c_2 2^{-N}) \cup (-1/2 + c_2 2^{-N}, -1/2 + c_1 2^{-N}). \quad (3.6)$$

Provided $N \geq 3$, we obtain

$$\int_{\Omega} |\nabla \Delta^{-1} \text{div}(\mathbf{u} \xi)|^2 d\mathbf{x} \lesssim \frac{1}{2^N \min\{d_x^2, d_y^2, 1\}}, \quad (3.7)$$

using the following proposition.

Proposition 3.2. *Let $f \in L^\infty(\Omega)$ such that $\text{supp}_z f \subseteq (1/2 - c_1 \varepsilon, 1/2 - c_2 \varepsilon) \cup (-1/2 + c_2 \varepsilon, -1/2 + c_1 \varepsilon)$, where $0 < c_2 < c_1 < 1$ and $\varepsilon < 1/4$ are three constants, then we have*

$$\int_{\Omega} |\nabla \Delta^{-1} f|^2 d\mathbf{x} \lesssim \varepsilon^3 \|f\|_{L^\infty(\Omega)}^2. \quad (3.8)$$

Proof of the Proposition 3.2 is provided in section 5.

At this point, we prescribe n_x and n_y . As stated in the introduction, we have chosen $l_x \leq l_y$ without the loss of generality. We divide the proof of the theorem into two parts: (i) when $l_x \geq 1$, (ii) when $l_x < 1$.

In the first case ($l_x \geq 1$), we choose

$$n_x = \lceil l_x \rceil \quad \text{and} \quad n_y = \lceil l_y \rceil, \quad (3.9)$$

where $\lceil \cdot \rceil$ is the ceiling function. Then from the definitions of d_x and d_y , we have

$$\frac{1}{2} \leq d_x, d_y \leq 1. \quad (3.10)$$

Noting this and using the estimates (3.2), (3.3), (3.4) and (3.5) in (1.11) gives

$$\frac{1}{c_5 \frac{1}{2^N} + c_6 \frac{4^N}{\mathcal{P}}} \lesssim Q_{\max}(\mathcal{P}), \quad (3.11)$$

where c_5 and c_6 are two constants independent of any parameter. Choosing the value of N as

$$N = \left\lceil \frac{1}{3} \log_2 \frac{c_5 \mathcal{P}}{2c_6} \right\rceil, \quad (3.12)$$

we can show

$$\mathcal{P}^{1/3} \lesssim Q_{\max}(\mathcal{P}) \quad (3.13)$$

provided

$$\mathcal{P} \gtrsim \frac{2c_6}{c_5}. \quad (3.14)$$

In the second case, when $l_x < 1$, we choose

$$n_x = 1 \quad \text{and} \quad n_y = \left\lceil \frac{l_y}{l_x} \right\rceil, \quad (3.15)$$

then we have

$$d_x = l_x \quad \text{and} \quad \frac{l_x}{2} \leq d_y \leq l_x. \quad (3.16)$$

The estimates (3.2), (3.3), (3.4) and (3.5) then imply

$$\frac{1}{c_7 \frac{1}{2^N l_x^2} + c_8 \frac{4^N}{\mathcal{P} l_x^4}} \lesssim Q_{\max}(\mathcal{P}), \quad (3.17)$$

for some positive constants c_7 and c_8 independent of any parameter. Now choosing the following value of N

$$N = \left\lceil \frac{1}{3} \log_2 \frac{c_7 \mathcal{P} l_x^2}{2c_8} \right\rceil, \quad (3.18)$$

we obtain

$$\mathcal{P}^{1/3} l_x^{8/3} \lesssim Q_{\max}(\mathcal{P}), \quad (3.19)$$

provided

$$\mathcal{P} \gtrsim \frac{2c_8}{c_7 l_x^2}, \quad (3.20)$$

which then completes the proof of the Theorem 1.1. \square

4 Construction of three-dimensional branching pipe flow: Step I and Step II

The goal of this section is to perform Step I, which is to build the parent constructs $\bar{\mathbf{u}}$, $\bar{\mathbf{u}}_b$, $\bar{\xi}$ and $\bar{\xi}_b$, followed by Step II, which is to create the main copies $\bar{\mathbf{u}}_N$ and $\bar{\xi}_N$. We start by giving a sketch of the parent copies and how to assemble their dilated versions to create the main copies, which is then followed by the actual construction in Step I and Step II.

4.1 A detailed sketch of the construction

As the support of the velocity field $\bar{\mathbf{u}}_N$ looks like a pipe network (see figure 4) and the flow field itself is similar to flow in pipes, we use words such as pipe, pipe network or pipeline for ease of exposition below.

The main copy $\bar{\mathbf{u}}_N$ consists of two “pipelines”: one in which the flow goes upward (the positive z -direction) in a branching fashion, \mathbf{P}_{up} (shown in red in figure 4) and one in which the flow goes downward (the negative z -direction), again in a branching fashion, \mathbf{P}_{down} (shown in blue). The part of the pipelines \mathbf{P}_{up} and \mathbf{P}_{down} that resides in the parent construct $\bar{\mathbf{u}}$ is also shown in red and blue, in figure 3.

The volume flow rate through both of these pipelines is the same. In what follows, we describe the pipeline design only for $z \geq 0$ and simply use mirror symmetry to construct the pipeline for $z \leq 0$. In the parent

construct, \mathbf{P}_{up} starts from a center pipe, denoted by P_c in figure 3a. The center pipe goes up vertically, until a first junction at $z = 1/8$, where it splits into four pipes going right (positive x -direction) P_r , left (negative x -direction) P_l , front (positive y -direction) P_f and back (negative y -direction) P_b . In plumbing terms, the junction of these pipes would be known as a 5-way cross. The horizontal extent of these pipes is $1/4$. Near the junction, each of the four horizontal pipes has a radius equal to that of P_c . Therefore, because of incompressibility condition, the speed of the flow goes down by a factor of four as the flow enters from P_c to P_r , P_l , P_f and P_b . However, away from the junction (midway), a constriction is added to reduce the radii of these four pipes by a factor of half after which the speed of the flow regains its original value (again because of incompressibility). In plumbing terms, the region where the radius of the pipe decreases is known as a reducer. Finally, these horizontal pipes bend upward up to a level $z = 1/4$. With this construction, the pipeline \mathbf{P}_{up} near $z = 1/4$ consists of four pipes whose radius is half that of the pipe P_c near $z = 0$ but all of them with same magnitude of velocity. We can then continue the pipeline from $z = 1/4$ to $z = 1/4 + 1/8$ by adding four half-sized copies of the original one. In a similar way, the pipeline can be further continued up to any number of levels N .

The pipeline in which the flow goes down consists of four pipes surrounding P_c , each with radii equal to that of P_c . The speed of the flow in one of these four pipes is $1/4$ the speed of the flow in P_c , ensuring that the total volume flow going upward and downward are the same. The flow in these four pipes come from the horizontally placed pipes that are similarly surrounding the pipes P_r , P_l , P_f and P_b as shown in figure 3a. The radii of these horizontal pipes, similar to the case of the previous pipeline, changes by a factor of two to ensure that the flow velocity in the vertical pipes that they connect remains the same. Finally, before bending in the upward direction, the horizontal pipes, in this pipeline, close their distance to the horizontal pipes from pipeline \mathbf{P}_{up} to make sure that we can glue a self-similar parent copy of half-the-size to continue the pipeline.

The self-similar continuation of both pipelines truncates after a fixed number of levels N (depending on \mathcal{P}). In the last level (closest to the wall), the two pipelines merge, i.e., the flow from the pipeline \mathbf{P}_{up} goes to the pipeline \mathbf{P}_{down} . This done by gluing an appropriately scaled parent construct $\bar{\mathbf{u}}_b$ as shown in figure 3c.

Once we have the main copy $\bar{\mathbf{u}}_N$ ready, we can select $\bar{\xi}_N$. We choose $\bar{\xi}_N$ (everywhere except in the boundary layers where the pipelines truncate) to be such that its value is a positive constant ξ_0 in the region where the pipeline \mathbf{P}_{up} lies and is $-\xi_0$ in the region where the pipeline \mathbf{P}_{down} lies and decays to zero rapidly away from these pipelines (see figure 4). There are two advantages with this choice:

- (i) The quantity $\bar{\mathbf{u}}_N \cdot \nabla \bar{\xi}_N$ is identically zero except in the last level of construction where the branching structure truncates. Therefore, it is possible to restrict the support of $\bar{\mathbf{u}}_N \cdot \nabla \bar{\xi}_N$ to a thin horizontal layer close to the wall, which helps in obtaining a good estimate on the nonlocal term in (1.12a-c).
- (ii) The transport term simplifies as follows.

$$\int \bar{\mathbf{u}}_{N,z} \bar{\xi}_N d\mathbf{x} \approx \xi_0 \int_{\mathbf{P}_{up}} \bar{\mathbf{u}}_{N,z} d\mathbf{x} - \xi_0 \int_{\mathbf{P}_{down}} \bar{\mathbf{u}}_{N,z} d\mathbf{x} \approx 2\xi_0 V_0,$$

where $V_0 > 0$ is the total flow (constant volume flux through any horizontal section) going upward in pipeline \mathbf{P}_{up} or downward in pipeline \mathbf{P}_{down} . There will be minor corrections in the region where the pipelines truncate, which is why we use the approximate symbol.

In summary, we built two pipelines with a self-similar “tree-like” branching structure. The first one, \mathbf{P}_{up} , is “hot” (as $\bar{\xi}_N$ is positive in that region) in which the flow goes up and the second one, \mathbf{P}_{down} , is “cold” (as $\bar{\xi}_N$ is negative) and surrounds (without touching) the hot pipeline \mathbf{P}_{up} . This type of “disentanglement” of the hot pipeline from the cold one is possible in three dimensions but not in two dimensions and is the main reason behind the proof of Theorem 1.1.

4.2 Step I: Construction of the parent copies

The purpose of this subsection is to build the parent constructs: $\bar{\mathbf{u}}$, $\bar{\mathbf{u}}_b$ and the trial ξ -field: $\bar{\xi}$, $\bar{\xi}_b$. Let us define a few parameters that will be frequently used in this section:

$$\gamma = \frac{1}{500}, \quad \lambda = \frac{1}{100}, \quad \delta = \frac{1}{20}. \quad (4.1)$$

These parameters can roughly be understood as follows. The parameter γ can be thought of as the radius of pipes in which the flow field is supported, whereas λ is the radius of pipes in which the ξ -field is supported and δ denotes the distance between pipeline \mathbf{P}_{up} and \mathbf{P}_{down} in the parent copy $\overline{\mathbf{u}}$.

4.2.1 The flow field $\overline{\mathbf{u}}$ and $\overline{\mathbf{u}}_b$

To construct the flow field, the basic idea is to define an appropriate vector-valued Radon measure supported on a set. This set is a collection of line segments and rays, which, in a loose sense, form the skeleton of the pipelines whose sketch is described in subsection 4.1. Most of the desired flow field will then be created by regularizing the Radon measure using a convolution with a mollifier, except in the reducer region of the pipelines. The flow field in the reducer region will be designed separately with the help of an axisymmetric streamfunction.

We start by defining a few important points in \mathbb{R}^3 , which will be helpful in creating the “skeleton” of the pipelines. We define

$$\mathbf{p}_1 := (0, 0, 0), \quad \mathbf{p}_2 := (0, 0, 1/8), \quad \mathbf{p}_3 := (1/4, 0, 1/8), \quad \mathbf{p}_4 := (1/4, 0, 1/4),$$

and

$$\begin{aligned} \mathbf{q}_1^{i,j} &:= (\delta, j\delta, 0), \quad \mathbf{q}_2^{i,j} := (\delta, j\delta, 1/8 - i\delta), \quad \mathbf{q}_3^{i,j} := \left(\frac{1}{4} + \frac{i\delta}{2}, j\delta, 1/8 - i\delta\right), \\ \mathbf{q}_4^{i,j} &:= \left(\frac{1}{4} + \frac{i\delta}{2}, \frac{j\delta}{2}, 1/8 - i\delta\right), \quad \mathbf{q}_5^{i,j} := \left(\frac{1}{4} + \frac{i\delta}{2}, \frac{j\delta}{2}, \frac{1}{4}\right), \end{aligned}$$

where $i, j \in \mathbb{Z}$. Next, we define a family of points, obtained by horizontal rotation of the points defined above. Let $\theta \in [0, 2\pi]$, we define

$$\mathbf{p}_{k,\theta} := \rho_\theta(\mathbf{p}_k) \quad \text{for } k \in \{1, 2, 3, 4\}; \quad \mathbf{q}_{k,\theta}^{i,j} := \rho_\theta(\mathbf{q}_k^{i,j}) \quad \text{for } k \in \{1, 2, 3, 4, 5\}. \quad (4.2)$$

We recall that the transformation ρ_θ , defined in section 2, is a counterclockwise horizontal rotation by an angle θ .

We define two sets:

$$J := \{-1, 1\} \quad \text{and} \quad \Theta := \left\{0, \frac{\pi}{2}, \pi, \frac{3\pi}{2}\right\}.$$

Before defining the appropriate vector-valued Radon measures, we set a few notations. Given two points $\mathbf{a}_1, \mathbf{a}_2 \in \mathbb{R}^3$, where $\mathbf{a}_1 \neq \mathbf{a}_2$, we denote the line segment whose end points are \mathbf{a}_1 and \mathbf{a}_2 as

$$\overline{\mathbf{a}_1 \mathbf{a}_2} := \{(1-t)\mathbf{a}_1 + t\mathbf{a}_2 \mid t \in [0, 1]\}, \quad (4.3)$$

whereas to denote the ray that starts at \mathbf{a}_1 and goes all the way up to infinity, passing through the point \mathbf{a}_2 as

$$\overrightarrow{\mathbf{a}_1 \mathbf{a}_2} := \{(1-t)\mathbf{a}_1 + t\mathbf{a}_2 \mid t \in [0, \infty)\}. \quad (4.4)$$

For a given $S \subseteq \mathbb{R}^3$ and $\varepsilon > 0$, we denote the ε -neighborhood of the set S by

$$S^\varepsilon := \{\mathbf{x} \in \mathbb{R}^3 \mid \text{dist}(\mathbf{x}, S) \leq \varepsilon\}. \quad (4.5)$$

Finally, \mathcal{H}^1 denotes the Hausdorff measure of dimension one.

Using Table 1, we now define a few vector-valued measures as

$$\nu^u := \nu_0 + \nu_1 + \nu_2, \quad (4.7a)$$

$$\nu^d := \nu_3 + \nu_4 + \nu_5 + \nu_6 + \nu_7, \quad (4.7b)$$

$$\nu^b := \nu_0 + \nu_8 + \nu_9. \quad (4.7c)$$

$\ell_0 := \overrightarrow{p_2 p_1}$	$e_0 := e_z$	$\nu_0 := e_0 \mathcal{H}^1 \llcorner \ell_0$	(4.6a)
$\ell_{1,\theta} := \overrightarrow{p_{2,\theta} p_{3,\theta}}$	$e_{1,\theta} := \frac{1}{4} \frac{p_{3,\theta} - p_{2,\theta}}{ p_{3,\theta} - p_{2,\theta} }$	$\nu_1 := \sum_{\theta \in \Theta} e_{1,\theta} \mathcal{H}^1 \llcorner \ell_{1,\theta}$	(4.6b)
$\ell_{2,\theta} := \overrightarrow{p_{3,\theta} p_{4,\theta}}$	$e_{2,\theta} := \frac{e_z}{4}$	$\nu_2 := \sum_{\theta \in \Theta} e_{2,\theta} \mathcal{H}^1 \llcorner \ell_{2,\theta}$	(4.6c)
$\ell_{3,\theta} := \overrightarrow{q_{2,\theta}^{1,1} q_{1,\theta}^{0,1}}$	$e_{3,\theta} := -\frac{e_z}{4}$	$\nu_3 := \sum_{\theta \in \Theta} e_{3,\theta} \mathcal{H}^1 \llcorner \ell_{3,\theta}$	(4.6d)
$\ell_{4,\theta} := \overrightarrow{q_{2,\theta}^{-1,1} q_{2,\theta}^{1,1}}$	$e_{4,\theta} := -\frac{e_z}{8}$	$\nu_4 := \sum_{\theta \in \Theta} e_{4,\theta} \mathcal{H}^1 \llcorner \ell_{4,\theta}$	(4.6e)
$\ell_{5,\theta}^{i,j} := \overrightarrow{q_{2,\theta}^{i,j} q_{3,\theta}^{i,j}}$	$e_{5,\theta}^{i,j} := \frac{1}{16} \frac{q_{2,\theta}^{i,j} - q_{3,\theta}^{i,j}}{ q_{2,\theta}^{i,j} - q_{3,\theta}^{i,j} }$	$\nu_5 := \sum_{\theta \in \Theta} \sum_{i,j \in J} e_{5,\theta}^{i,j} \mathcal{H}^1 \llcorner \ell_{5,\theta}^{i,j}$	(4.6f)
$\ell_{6,\theta}^{i,j} := \overrightarrow{q_{3,\theta}^{i,j} q_{4,\theta}^{i,j}}$	$e_{6,\theta}^{i,j} := \frac{1}{16} \frac{q_{3,\theta}^{i,j} - q_{4,\theta}^{i,j}}{ q_{3,\theta}^{i,j} - q_{4,\theta}^{i,j} }$	$\nu_6 := \sum_{\theta \in \Theta} \sum_{i,j \in J} e_{6,\theta}^{i,j} \mathcal{H}^1 \llcorner \ell_{6,\theta}^{i,j}$	(4.6g)
$\ell_{7,\theta}^{i,j} := \overrightarrow{q_{4,\theta}^{i,j} q_{5,\theta}^{i,j}}$	$e_{7,\theta}^{i,j} := -\frac{e_z}{16}$	$\nu_7 := \sum_{\theta \in \Theta} \sum_{i,j \in J} e_{7,\theta}^{i,j} \mathcal{H}^1 \llcorner \ell_{7,\theta}^{i,j}$	(4.6h)
$\ell_{8,\theta} := \overrightarrow{q_{2,\theta}^{0,1} q_{1,\theta}^{0,1}}$	$e_{8,\theta} := -\frac{e_z}{4}$	$\nu_8 := \sum_{\theta \in \Theta} e_{8,\theta} \mathcal{H}^1 \llcorner \ell_{8,\theta}$	(4.6i)
$\ell_{9,\theta} := \overrightarrow{p_2 q_{2,\theta}^{0,1}}$	$e_{9,\theta} := \frac{1}{4} \frac{q_{2,\theta}^{0,1} - p_2}{ q_{2,\theta}^{0,1} - p_2 }$	$\nu_9 := \sum_{\theta \in \Theta} e_{9,\theta} \mathcal{H}^1 \llcorner \ell_{9,\theta}$	(4.6j)

Table 1: A few useful definitions: line segments or rays (column one), vectors in \mathbb{R}^3 (column two) and vector-valued measures (column three).

The measure ν^u will be used in constructing the upward moving part of the flow field $\overline{\mathbf{u}}$ and ν^d will be used for constructing the downward moving part of the flow field, whereas, ν_b will be useful in constructing the flow field $\overline{\mathbf{u}}_b$. We also define a few useful sets as

$$S^u := \ell_0 \cup \bigcup_{\theta \in \Theta} \ell_{1,\theta} \cup \ell_{2,\theta}, \quad (4.8a)$$

$$S^d := \bigcup_{\theta \in \Theta} \left(\ell_{3,\theta} \cup \ell_{4,\theta} \cup \bigcup_{i,j \in J} \ell_{5,\theta}^{i,j} \cup \ell_{6,\theta}^{i,j} \cup \ell_{7,\theta}^{i,j} \right), \quad (4.8b)$$

$$S := S^u \cup S^d, \quad (4.8c)$$

$$S_b := \ell_0 \cup \bigcup_{\theta \in \Theta} \ell_{8,\theta} \cup \ell_{9,\theta}. \quad (4.8d)$$

To regularize the measures, we define a family of mollifiers. Let $\varphi \in C_c^\infty(\mathbb{R}^3)$ be any radial bump function whose support lies in $|\mathbf{x}| \leq 1$, such as

$$\varphi(\mathbf{x}) := \overline{\varphi}(|\mathbf{x}|), \quad (4.9)$$

where $\overline{\varphi} : \mathbb{R} \rightarrow \mathbb{R}$ is defined as

$$\overline{\varphi}(r) := \begin{cases} c \exp\left(\frac{1}{r^2-1}\right) & \text{if } |r| < 1, \\ 0 & \text{if } |r| \geq 1, \end{cases} \quad (4.10)$$

and c is chosen such that $\int_{\mathbb{R}^3} \varphi(\mathbf{x}) d\mathbf{x} = 1$. For any $\varepsilon > 0$, we then define a standard mollifier as

$$\varphi_\varepsilon(\mathbf{x}) := \frac{1}{\varepsilon^3} \varphi\left(\frac{\mathbf{x}}{\varepsilon}\right). \quad (4.11)$$

We use this definition of mollifier and the measures (4.7a-d) to define the velocity fields

$$\left. \begin{aligned} \overline{\mathbf{u}}_1^u &:= \varphi_\gamma * \nu^u, & \overline{\mathbf{u}}_2^u &:= \varphi_{\frac{\gamma}{2}} * \nu^u, \\ \overline{\mathbf{u}}_1^d &:= \varphi_\gamma * \nu^d, & \overline{\mathbf{u}}_2^d &:= \varphi_{\frac{\gamma}{2}} * \nu^d, \\ \overline{\mathbf{u}}_b &:= \varphi_\gamma * \nu_b. \end{aligned} \right\} \quad (4.12a-e)$$

From the definition of φ_ε in (4.11) and the definition of the velocity fields (4.12a-e), we see that

$$\left. \begin{aligned} \text{supp } \overline{\mathbf{u}}_1^u \cup \text{supp } \overline{\mathbf{u}}_2^u &\subseteq S^{u,\gamma}, & \text{supp } \overline{\mathbf{u}}_1^d \cup \text{supp } \overline{\mathbf{u}}_2^d &\subseteq S^{d,\gamma}, \\ \text{supp } \overline{\mathbf{u}}_b &\subseteq S_b^\gamma. \end{aligned} \right\} \quad (4.13a-c)$$

Here, we added γ in the superscripts to mean γ -neighborhood of the sets (see definition (4.5)). Also, from the definition (4.12a-e), we see that all the velocity fields belong to $L^\infty(\mathbb{R}^3; \mathbb{R}^3)$.

Our next task is to show that the velocity fields as defined in (4.12a-e) belong to $C^\infty(\mathbb{R}^3; \mathbb{R}^3)$ and are divergence free. We start with the following definition.

Definition 4.1 (Kirchhoff's junction). Let $\widehat{\mathbf{p}} \in \mathbb{R}^3$ be a point and $\widehat{\mathbf{e}}_j \in \mathbb{R}^3$, for $j = 1$ to $n \in \mathbb{N}$, be different non-zero vectors. Also, let $o_j \in \{-1, 1\}$, for $j \in \{1, \dots, n\}$, be n numbers. We say $\widehat{\mathbf{p}}$ together with the set of pairs $\widehat{\mathbf{e}}_j$ and o_j forms a Kirchhoff's junction if

$$\sum_{j=1}^n o_j |\widehat{\mathbf{e}}_j| = 0. \quad (4.14)$$

For every Kirchhoff's junction defined above, we can associate a vector-valued Radon measure $\widehat{\nu}$. First define n rays emanating from $\widehat{\mathbf{p}}$ as $\widehat{\ell}_j := \{\mathbf{y}_j(t) \mid t \in [0, \infty)\}$, where $\mathbf{y}_j : \mathbb{R} \rightarrow \mathbb{R}^3$ are curves which in the parametric form are given by $\mathbf{y}_j(t) := \widehat{\mathbf{p}} + t\widehat{\mathbf{e}}_j/|\widehat{\mathbf{e}}_j|$, for $t \in [0, \infty)$. Consider the vector-valued Radon measures supported on these rays as $\widehat{\nu}_j := o_j \widehat{\mathbf{e}}_j \mathcal{H}^1 \llcorner \widehat{\ell}_j$. Using these measures, we define a measure corresponding to the Kirchhoff's junction as

$$\widehat{\nu} := \sum_{j=1}^n \widehat{\nu}_j. \quad (4.15)$$

Next, we state an important lemma.

Lemma 4.1. Let $\psi \in C_c^\infty(\mathbb{R}^3)$ be a radially symmetric mollifier such that the support of ψ lies in $|\mathbf{x}| \leq \varepsilon$, for some $\varepsilon > 0$. Assume that $\widehat{\mathbf{p}} \in \mathbb{R}^3$ and a set of n pairs, $\widehat{\mathbf{e}}_j \in \mathbb{R}^3$ and $o_j \in \{-1, 1\}$, for $j = 1$ to $n \in \mathbb{N}$, forms a Kirchhoff's junction. Let $\widehat{\nu}$ be the associated vector-valued Radon measure to this junction. Then the velocity field given by $\widehat{\mathbf{u}} := \psi * \widehat{\nu}$ belongs to $C^\infty(\mathbb{R}^3; \mathbb{R}^3)$ and is divergence-free.

Proof of Lemma 4.1. By differentiating under the integral sign in the expression of $\widehat{\mathbf{u}}$, we immediately see that

$\hat{\mathbf{u}} \in C^\infty(\mathbb{R}^3; \mathbb{R}^3)$. Next, for any $\mathbf{x}_0 \in \mathbb{R}^3$, the following calculation holds

$$\begin{aligned} (\nabla \cdot \hat{\mathbf{u}})(\mathbf{x}_0) &= \sum_{j=1}^n o_j \int_{\mathbb{R}^3} \hat{\mathbf{e}}_j \cdot \nabla \psi(\mathbf{x}_0 - \mathbf{y}) d\mathcal{H}^1 \llcorner \hat{\ell}_j(\mathbf{y}) = \sum_{j=1}^n o_j \int_0^\infty \hat{\mathbf{e}}_j \cdot \nabla \psi(\mathbf{x}_0 - \mathbf{y}_j(t_j)) dt_j \\ &= - \sum_{j=1}^n o_j |\hat{\mathbf{e}}_j| \int_0^\infty \frac{\partial \psi(\mathbf{x}_0 - \mathbf{y}_j(t_j))}{\partial t_j} dt_j = - \sum_{j=1}^n o_j |\hat{\mathbf{e}}_j| \psi(\mathbf{x}_0 - \mathbf{y}_j(t_j))|_0^\infty = \psi(\hat{\mathbf{p}}) \sum_{j=1}^n o_j |\hat{\mathbf{e}}_j|. \end{aligned}$$

Finally, using the assumption of the Kirchhoff's junction, implies $\nabla \cdot \hat{\mathbf{u}} \equiv 0$. \square

Corollary 4.1. *Let $\psi \in C_c^\infty(\mathbb{R}^3)$ be a radially symmetric mollifier such that the support of ψ lies in $|\mathbf{x}| \leq \varepsilon$, for some $\varepsilon > 0$. Let $\hat{\mathbf{p}}_i \in \mathbb{R}^3$, where $i \in \{1, \dots, m\}$, be m points which are part of m different Kirchhoff's junctions and let $\hat{\nu}_i$ be the vector-valued Radon measures associated to each of the Kirchhoff's junction. Then for the vector-valued Radon measure defined as $\check{\nu} := \sum_{i=1}^m \hat{\nu}_i$, the velocity field given by $\check{\mathbf{u}} := \psi * \check{\nu}$ belongs to $C^\infty(\mathbb{R}^3; \mathbb{R}^3)$ and is divergence-free.*

Lemma 4.2. *Let $\hat{\mathbf{p}}_1$ and $\hat{\mathbf{p}}_2$ be two different points in \mathbb{R}^3 . Let $\hat{\ell}_{12} = \overline{\hat{\mathbf{p}}_1 \hat{\mathbf{p}}_2}$ and $\hat{\mathbf{e}}_{12} = c(\hat{\mathbf{p}}_2 - \hat{\mathbf{p}}_1)$ for some $c > 0$. Then a vector-valued measure defined as $\hat{\nu}_{12} := \hat{\mathbf{e}}_{12} \mathcal{H}^1 \llcorner \hat{\ell}_{12}$ can also be written as $\hat{\nu}_{12} = \hat{\nu}_{in} + \hat{\nu}_{out}$, where $\hat{\nu}_{in} = (-\hat{\mathbf{e}}_{12}) \mathcal{H}^1 \llcorner \hat{\ell}_{in}$, $\hat{\nu}_{out} = \hat{\mathbf{e}}_{12} \mathcal{H}^1 \llcorner \hat{\ell}_{out}$, $\hat{\ell}_{in} = \{\hat{\mathbf{p}}_2 + t\hat{\mathbf{e}}_{12} \mid t \in [0, \infty)\}$, and $\hat{\ell}_{out} = \{\hat{\mathbf{p}}_1 + t\hat{\mathbf{e}}_{12} \mid t \in [0, \infty)\}$.*

Proof of 4.2. We can write $\hat{\nu}_{out} = \hat{\nu}_{out} \llcorner \hat{\ell}_{12} + \hat{\nu}_{out} \llcorner \hat{\ell}_{in}$. Now $\hat{\nu}_{out} \llcorner \hat{\ell}_{12}$ coincides with $\hat{\nu}_{12}$ in \mathbb{R}^3 , whereas $\hat{\nu}_{in} + \hat{\nu}_{out} \llcorner \hat{\ell}_{in}$ is a zero measure, which then finishes the proof. \square

A tedious verification shows that using Lemma 4.2, the vector-valued measures (4.7a-c) can be written as a sum of vector-valued measures associated with different Kirchhoff's junctions. Therefore, the velocity fields as defined in (4.12a-e) belong to $C^\infty(\mathbb{R}^3; \mathbb{R}^3)$ and are divergence free. Here, we write down the Kirchhoff's junctions such that the sum of associated vector-valued measures is ν^u :

Junction No.	The point $\hat{\mathbf{p}}$	The set of pairs of $\hat{\mathbf{e}}_j$ and o_j
1	\mathbf{p}_2	$\{(e_z, 1), (\frac{e_x}{4}, -1), (\frac{e_y}{4}, -1), (-\frac{e_x}{4}, -1), (-\frac{e_y}{4}, -1)\}$
2	$\mathbf{p}_{3,0}$	$\{(-\frac{e_x}{4}, 1), (\frac{e_x}{4}, -1)\}$
3	$\mathbf{p}_{3,\frac{\pi}{2}}$	$\{(-\frac{e_y}{4}, 1), (\frac{e_z}{4}, -1)\}$
4	$\mathbf{p}_{3,\pi}$	$\{(\frac{e_x}{4}, 1), (\frac{e_x}{4}, -1)\}$
5	$\mathbf{p}_{3,\frac{3\pi}{2}}$	$\{(\frac{e_y}{4}, 1), (\frac{e_z}{4}, -1)\}$

It can be shown that a similar decomposition exists for the other three measures defined in (4.7).

4.2.1.1 Patching up $\bar{\mathbf{u}}_1$ and $\bar{\mathbf{u}}_2$: Construction in the reducer region

To design the velocity field $\bar{\mathbf{u}}$, we need to patch the velocity fields $\bar{\mathbf{u}}_1$ and $\bar{\mathbf{u}}_2$ by defining an appropriate velocity field in the reducer region. Therefore, at this point, we shift our focus to designing velocity field in the reducer region.

We start by considering a simple example of one reducer, where we design such a velocity field. Let's define a function $m : \mathbb{R} \rightarrow \mathbb{R}$ as

$$m(r) := \frac{1}{\gamma^3} \int_{-\infty}^{\infty} \bar{\varphi} \left(\frac{\sqrt{x'^2 + r^2}}{\gamma} \right) dx', \quad (4.16)$$

where $\bar{\varphi}$ is defined in (4.10). In what follows, we will use

$$\varrho \text{ as a placeholder for } \sqrt{y^2 + z^2}$$

in rest of the section. With these definitions in hand, we define two velocity fields $\bar{\mathbf{u}}_s, \bar{\mathbf{u}}_e : \mathbb{R}^3 \rightarrow \mathbb{R}^3$ as

$$\bar{\mathbf{u}}_s(\mathbf{x}) := (\bar{u}_{x,s}, \bar{u}_{y,s}, \bar{u}_{z,s}) := (m(\varrho), 0, 0), \quad \bar{\mathbf{u}}_e(\mathbf{x}) := (\bar{u}_{x,e}, \bar{u}_{y,e}, \bar{u}_{z,e}) := (4m(2\varrho), 0, 0) \quad \text{for } \mathbf{x} \in \mathbb{R}^3. \quad (4.17)$$

As φ has a compact support, therefore, $\bar{\mathbf{u}}_s, \bar{\mathbf{u}}_e \in L^\infty(\mathbb{R}^3; \mathbb{R}^3)$. The arguments given in Appendix C show that both of these velocity fields also belong to $C^\infty(\mathbb{R}^3; \mathbb{R}^3)$. Furthermore, it is clear that both the velocity fields are divergence free. Finally, one can verify that the volume flux through any plane parallel to the yz -plane is same for both the velocity fields.

The task at hand is to come up with a divergence free velocity field $\bar{\mathbf{u}}_c$ such that it coincides with \mathbf{u}_s in the region $x \leq 0$ and it coincides with \mathbf{u}_e in the region $\gamma \leq x$, and it belongs to $L^\infty(\mathbb{R}^3; \mathbb{R}^3) \cap C^\infty(\mathbb{R}^3; \mathbb{R}^3)$. To ensure the required velocity field is divergence free, we work with streamfunctions. The strategy is to define the velocity field in the reducer region ($0 < x < \gamma$) based on a streamfunction which smoothly matches with streamfunction corresponding to the velocity field \mathbf{u}_s for $x \leq 0$ and with streamfunction corresponding to the velocity field \mathbf{u}_e for $x \geq \gamma$. To pursue this idea, we define two functions $\Psi_s, \Psi_e : \mathbb{R} \rightarrow \mathbb{R}$ as

$$\Psi_s(r) := \int_0^{|r|} r' m(r') dr', \quad \Psi_e(r) := 4 \int_0^{|r|} r' m(2r') dr'.$$

Next, we define $\Psi_c : \mathbb{R}^2 \rightarrow \mathbb{R}$ as

$$\Psi_c(x, r) := (1 - \eta_\gamma(x))\Psi_s(r) + \eta_\gamma(x)\Psi_e(r),$$

where $\eta_\varepsilon = \eta(x/\varepsilon)$ and η is a smooth cut-off function such that $\eta \equiv 0$ for $x \leq 0$ and $\eta \equiv 1$ for $x \geq 1$.

The function $\Psi_c(x, r)$ may be understood as the axisymmetric streamfunction of the desired velocity field. With the help of $\Psi_c(x, r)$, we are ready to define the components of the velocity field that we wish to construct as

$$\begin{aligned} \bar{u}_{x,c}(\mathbf{x}) &:= (1 - \eta_\gamma(x))m(\varrho) + 4m(2\varrho)\eta_\gamma(x) \\ \bar{u}_{y,c}(\mathbf{x}) &:= \begin{cases} y \frac{d\eta_\gamma}{dx} \frac{1}{\varrho^2} (\Psi_s(\varrho) - \Psi_e(\varrho)) & \text{if } \varrho \neq 0, \\ 0 & \text{if } y, z = 0. \end{cases} \\ \bar{u}_{z,c}(\mathbf{x}) &:= \begin{cases} z \frac{d\eta_\gamma}{dx} \frac{1}{\varrho^2} (\Psi_s(\varrho) - \Psi_e(\varrho)) & \text{if } \varrho \neq 0, \\ 0 & \text{if } y, z = 0. \end{cases} \end{aligned}$$

where $\mathbf{x} \in \mathbb{R}^3$. The velocity field is then given by

$$\bar{\mathbf{u}}_c := (\bar{u}_{x,c}, \bar{u}_{y,c}, \bar{u}_{z,c}). \quad (4.18)$$

With this definition, we state the following lemma.

Lemma 4.3. *Let the velocity field $\bar{\mathbf{u}}_c$ be as defined in (4.18). Then it coincides with $\bar{\mathbf{u}}_s$ when $x \leq 0$ and with $\bar{\mathbf{u}}_e$ when $\gamma \leq x$. Furthermore, $\bar{\mathbf{u}}_c \in L^\infty(\mathbb{R}^3; \mathbb{R}^3) \cap C^\infty(\mathbb{R}^3; \mathbb{R}^3)$ and is divergence free with*

$$\text{supp } \bar{\mathbf{u}}_c \subseteq \{(x, y, z) \mid y^2 + z^2 \leq \gamma^2\}. \quad (4.19)$$

Proof. With the definition of function m (4.16) and noting that $\Psi_s(\varrho) = \Psi_e(\varrho)$ when $\varrho > \gamma$, we obtain (4.19). It is clear by construction that $\bar{\mathbf{u}}_c$ coincides with $\bar{\mathbf{u}}_s$ when $x \leq 0$ and with $\bar{\mathbf{u}}_e$ when $\gamma \leq x$ and therefore it is also infinite differentiable in these regions. To see the infinite differentiability in the region $0 < x < \gamma$, we use Lemma 4.3 given in Appendix C. Finally, as the velocity field $\bar{\mathbf{u}}_c$ is defined based on a streamfunction, it is necessarily divergence-free. \square

With this lemma in hand, we are ready to patch $\bar{\mathbf{u}}_1$ and $\bar{\mathbf{u}}_2$ using $\bar{\mathbf{u}}_c$ to construct the velocity field $\bar{\mathbf{u}}$. For

this purpose, we define a few points in \mathbb{R}^3 as

$$\mathbf{s}_0 = (1/8, 0, 0), \quad \mathbf{s}_1^{i,j} = (1/8, j\delta, -i\delta) \quad \text{for } i, j \in J. \quad (4.20)$$

We also define two velocity field as

$$\overline{\mathbf{u}}_{red}^u := \frac{1}{4} T^{\mathbf{s}_0} \overline{\mathbf{u}}_c, \quad \overline{\mathbf{u}}_{red}^d := -\frac{1}{16} \sum_{i,j \in J} T^{\mathbf{s}_1^{i,j}} \overline{\mathbf{u}}_c.$$

As a result of Lemma 4.3, the velocity fields

$$\begin{aligned} \overline{\mathbf{u}}^u &:= \overline{\mathbf{u}}_1^u \mathbf{1}_{\{|x|, |y| \leq 1/8\}} + \overline{\mathbf{u}}_2^u \mathbf{1}_{\{|x| \geq 1/8+\gamma\} \cup \{|y| \geq 1/8+\gamma\}} + \sum_{\theta \in \Theta} \rho_\theta \overline{\mathbf{u}}_{red}^u \mathbf{1}_{\{1/8 < x < 1/8+\gamma\}}, \\ \overline{\mathbf{u}}^d &:= \overline{\mathbf{u}}_1^d \mathbf{1}_{\{|x|, |y| \leq 1/8\}} + \overline{\mathbf{u}}_2^d \mathbf{1}_{\{|x| \geq 1/8+\gamma\} \cup \{|y| \geq 1/8+\gamma\}} + \sum_{\theta \in \Theta} \rho_\theta \overline{\mathbf{u}}_{red}^d \mathbf{1}_{\{1/8 < x < 1/8+\gamma\}}, \end{aligned}$$

are uniformly bounded, infinitely differentiable, divergence free with $\text{supp } \overline{\mathbf{u}}^u \subseteq S^{u,\gamma}$ and $\text{supp } \overline{\mathbf{u}}^d \subseteq S^{d,\gamma}$. Finally, we arrive at the definition of the parent construct

$$\overline{\mathbf{u}} := \overline{\mathbf{u}}^u + \overline{\mathbf{u}}^d. \quad (4.21)$$

Summarizing the properties of the parent constructs $\overline{\mathbf{u}}$ and $\overline{\mathbf{u}}_b$ (from (4.12a-e)), we have $\overline{\mathbf{u}}, \overline{\mathbf{u}}_b \in C^\infty(\mathbb{R}^3; \mathbb{R}^3) \cap L^\infty(\mathbb{R}^3; \mathbb{R}^3)$, both obeying $\nabla \cdot \overline{\mathbf{u}} \equiv 0$ and $\nabla \cdot \overline{\mathbf{u}}_b \equiv 0$ with

$$\text{supp } \overline{\mathbf{u}} \subseteq S^\gamma, \quad \text{supp } \overline{\mathbf{u}}_b \subseteq S_b^\gamma. \quad (4.22)$$

Next, define a few points in \mathbb{R}^3 as

$$\boldsymbol{\tau}_\theta := \left(\frac{\cos \theta}{4}, \frac{\sin \theta}{4}, -\frac{1}{4} \right) \quad \text{for } \theta \in \Theta.$$

We now gather an important property of the parent constructs $\overline{\mathbf{u}}$ and $\overline{\mathbf{u}}_b$, which is that the velocity fields defined as

$$\tilde{\mathbf{u}} := \overline{\mathbf{u}}(x) \mathbf{1}_{\{z < 1/4\}} + \left(\sum_{\theta \in \Theta} T^{\boldsymbol{\tau}_\theta} \overline{\mathbf{u}}(2x) \right) \mathbf{1}_{\{z \geq 1/4\}}, \quad (4.23a)$$

$$\tilde{\mathbf{u}}_b := \overline{\mathbf{u}}_b(x) \mathbf{1}_{\{z < 1/4\}} + \left(\sum_{\theta \in \Theta} T^{\boldsymbol{\tau}_\theta} \overline{\mathbf{u}}_b(2x) \right) \mathbf{1}_{\{z \geq 1/4\}}, \quad (4.23b)$$

$$\tilde{\mathbf{u}}_r := \overline{\mathbf{u}}(x) \mathbf{1}_{z \geq 0} + (-\overline{u}_x(x, y, -z), -\overline{u}_y(x, y, -z), \overline{u}_z(x, y, -z)) \mathbf{1}_{z < 0}, \quad (4.23c)$$

all belong to $C^\infty(\mathbb{R}^3; \mathbb{R}^3)$. For example, let's look at $\tilde{\mathbf{u}}$. The infinite differentiability away from $z = 1/4$ is clear by definition. However, the velocity fields $\overline{\mathbf{u}}$ and

$$\sum_{\theta \in \Theta} T^{\boldsymbol{\tau}_\theta} \overline{\mathbf{u}}(2x)$$

are identical when $7/32 < z < 9/32$, which can be shown by writing down their explicit expressions in this region. Therefore, $\tilde{\mathbf{u}}$ is infinitely differentiable at $z = 1/4$ as well. Similar arguments apply for $\tilde{\mathbf{u}}_b$ and $\tilde{\mathbf{u}}_r$.

4.2.2 The scalar fields $\bar{\xi}$ and $\bar{\xi}_b$

The construction of $\bar{\xi}$ and $\bar{\xi}_b$ is relatively simple but somewhat different from that of $\overline{\mathbf{u}}$ and $\overline{\mathbf{u}}_b$. Recall from the detailed sketch given in section 4.1, we want to create a scalar field ξ that is constant in the support of the

velocity field \mathbf{u} (with the exception of the boundary layer). To that end, we first define a few sets consisting of line segments and rays, which in a sense form the skeleton. This step is the same as in the previous subsection. We then consider a λ -neighborhood of this skeleton for sufficiently small positive λ . Next, we mollify the indicator function of this λ -neighborhood set. If the mollification parameter, which we choose to be γ , is small compared with λ , we will have designed a smooth function supported in tubes of radius $\lambda + \gamma$ and constant in tubes of radius $\lambda - \gamma$ enveloping the skeleton. This strategy works everywhere except in the reducer region, where we design the scalar field using a cut-off function similar to the case of the velocity field. We now begin our construction.

In addition to (4.2), we define a few extra points in \mathbb{R}^3 as

$$\mathbf{p}_5 := (0, 0, h), \quad \mathbf{q}_6 := (\delta, \delta, h),$$

and a few rays

$$\ell_{10} := \overrightarrow{\mathbf{p}_5 \mathbf{p}_1}, \quad \ell_{11,\theta} := \overrightarrow{\mathbf{q}_{6,\theta} \mathbf{q}_{1,\theta}^{0,1}},$$

where $\mathbf{q}_{6,\theta} = \rho_\theta(\mathbf{q}_6)$. Here, we choose

$$h := \frac{1}{16}.$$

To complement (4.8), we also define

$$\tilde{S}_b^u := \ell_{10}, \quad \tilde{S}_b^d := \bigcup_{\theta \in \Theta} \ell_{11,\theta}.$$

Remember, we chose $\lambda = 1/100$ and $\gamma = 1/500$ (see (4.1)). Now using the definition of ε -neighborhood of a set (4.5), we define the following scalar fields:

$$\left. \begin{aligned} \bar{\xi}_1^u &:= \varphi_\gamma * \mathbf{1}_{S^{u,\lambda}}, & \bar{\xi}_1^d &:= -\varphi_\gamma * \mathbf{1}_{S^{d,\lambda}}, \\ \bar{\xi}_2^u &:= \varphi_{\gamma/2} * \mathbf{1}_{S^{u,\lambda/2}}, & \bar{\xi}_2^d &:= -\varphi_{\gamma/2} * \mathbf{1}_{S^{d,\lambda/2}}, \\ \bar{\xi}_b^u &:= \varphi_\gamma * \mathbf{1}_{\tilde{S}_b^{u,\lambda}}, & \bar{\xi}_b^d &:= -\varphi_\gamma * \mathbf{1}_{\tilde{S}_b^{d,\lambda}}, \end{aligned} \right\} \quad (4.24a-f)$$

which belong to $C^\infty(\mathbb{R}^3)$ as a result of the following lemma.

Lemma 4.4. *Let $f : \mathbb{R}^3 \rightarrow \mathbb{R}$ be a locally integrable function and let $\psi \in C_c^\infty(\mathbb{R}^3)$ be a radially symmetric mollifier such that the support of ψ lies in $|\mathbf{x}| \leq \epsilon$. Then the function given by $g = \psi * f$ belongs to $C^\infty(\mathbb{R}^3)$.*

Proof. By differentiating under the integral sign in the expression of g , one can finish the proof. \square

From the definitions (4.24a-f), we notice

$$\left. \begin{aligned} \text{supp } \bar{\xi}_1^u \cup \text{supp } \bar{\xi}_2^u &\subseteq S^{u,\lambda+\gamma}, & \text{supp } \bar{\xi}_1^d \cup \text{supp } \bar{\xi}_2^d &\subseteq S^{d,\lambda+\gamma}, \\ \text{supp } \bar{\xi}_b^u &\subseteq \tilde{S}_b^{u,\lambda+\gamma}, & \text{supp } \bar{\xi}_b^d &\subseteq \tilde{S}_b^{d,\lambda+\gamma}. \end{aligned} \right\} \quad (4.25a-d)$$

Moreover,

$$\left. \begin{aligned} \bar{\xi}_1^u(\mathbf{x}) = \bar{\xi}_2^u(\mathbf{x}) &= 1 \quad \text{when } \mathbf{x} \in S^{u,\frac{\lambda-\gamma}{2}}, & \bar{\xi}_1^d(\mathbf{x}) = \bar{\xi}_2^d(\mathbf{x}) &= -1 \quad \text{when } \mathbf{x} \in S^{d,\frac{\lambda-\gamma}{2}}, \\ \bar{\xi}_b^u(\mathbf{x}) &= 1 \quad \text{when } \mathbf{x} \in \tilde{S}_b^{u,\lambda-\gamma}, & \bar{\xi}_b^d(\mathbf{x}) &= -1 \quad \text{when } \mathbf{x} \in \tilde{S}_b^{d,\lambda-\gamma}. \end{aligned} \right\} \quad (4.26a-d)$$

Next, let's define two scalar fields for the construction in the reducer region

$$\begin{aligned}\bar{\xi}_{red}^u(\mathbf{x}) &:= \bar{\xi}_1^u(\mathbf{x})(1 - \eta_\gamma(x - 1/8)) + \bar{\xi}_2^u(\mathbf{x})\eta_\gamma(x - 1/8) \quad \text{for } \mathbf{x} \in \mathbb{R}^3, \\ \bar{\xi}_{red}^d(\mathbf{x}) &:= \bar{\xi}_1^d(\mathbf{x})(1 - \eta_\gamma(x - 1/8)) + \bar{\xi}_2^d(\mathbf{x})\eta_\gamma(x - 1/8) \quad \text{for } \mathbf{x} \in \mathbb{R}^3.\end{aligned}$$

We can use them to define

$$\begin{aligned}\bar{\xi}^u &:= \bar{\xi}_1^u \mathbf{1}_{\{|x|, |y| \leq 1/8\}} + \bar{\xi}_2^u \mathbf{1}_{\{|x|, |y| \geq 1/8+\gamma\}} + \sum_{\theta \in \Theta} \rho_\theta \bar{\xi}_{red}^u \mathbf{1}_{\{1/8 < x < 1/8+\gamma\}}, \\ \bar{\xi}^d &:= \bar{\xi}_1^d \mathbf{1}_{\{|x|, |y| \leq 1/8\}} + \bar{\xi}_2^d \mathbf{1}_{\{|x|, |y| \geq 1/8+\gamma\}} + \sum_{\theta \in \Theta} \rho_\theta \bar{\xi}_{red}^d \mathbf{1}_{\{1/8 < x < 1/8+\gamma\}}.\end{aligned}$$

It can be easily verified that $\bar{\xi}^u$ is infinitely differentiable, that its support lies in $S^{u, \lambda+\gamma}$ and that its value is 1 when $\mathbf{x} \in S^{u, \frac{\lambda-\gamma}{2}}$. Similarly, $\bar{\xi}^d$ is infinitely differentiable has a support that lies in $S^{d, \lambda+\gamma}$ and its value is -1 when $\mathbf{x} \in S^{d, \frac{\lambda-\gamma}{2}}$. We finally define the parent copies for the scalar field as

$$\bar{\xi} := \bar{\xi}^u + \bar{\xi}^d, \quad \bar{\xi}_b := \bar{\xi}_b^u + \bar{\xi}_b^d. \quad (4.29a-b)$$

In summary, $\bar{\xi}, \bar{\xi}_b \in L^\infty(\mathbb{R}^3) \cap C^\infty(\mathbb{R}^3)$, $\text{supp } \bar{\xi} \subseteq S^{u, \lambda+\gamma} \cup S^{d, \lambda+\gamma}$ and $\text{supp } \bar{\xi}_b \subseteq \tilde{S}_b^{u, \lambda+\gamma} \cup \tilde{S}_b^{d, \lambda+\gamma}$

Similar to the case of velocity field, an important outcome of our construction is that scalar fields

$$\tilde{\xi}(\mathbf{x}) := \bar{\xi}(\mathbf{x}) \mathbf{1}_{z < 1/4} + \sum_{\theta \in \Theta} T^{\tau_\theta}(\bar{\xi}(2\mathbf{x})) \mathbf{1}_{z \geq 1/4}, \quad (4.30a)$$

$$\tilde{\xi}_b(\mathbf{x}) := \bar{\xi}_b(\mathbf{x}) \mathbf{1}_{z < 1/4} + \sum_{\theta \in \Theta} T^{\tau_\theta}(\bar{\xi}_b(2\mathbf{x})) \mathbf{1}_{z \geq 1/4}, \quad (4.30b)$$

$$\tilde{\xi}_r(\mathbf{x}) := \bar{\xi}(\mathbf{x}) \mathbf{1}_{z \geq 0} + \bar{\xi}(x, y, -z) \mathbf{1}_{z < 0}, \quad (4.30c)$$

all belong to $C^\infty(\mathbb{R}^3)$.

Let's now gather some of the important properties of the parent constructs of the velocity field and the scalar field in the following proposition.

Proposition 4.2. *In the definitions (4.21, 4.12a-e) and (4.29a-b) the two velocity fields $\bar{\mathbf{u}}, \bar{\mathbf{u}}_b \in C^\infty(\mathbb{R}^3, \mathbb{R}^3) \cap L^\infty(\mathbb{R}^3, \mathbb{R}^3)$ and the scalar fields $\bar{\xi}, \bar{\xi}_b \in C^\infty(\mathbb{R}^3) \cap L^\infty(\mathbb{R}^3)$ are such that the following statements are true.*

- (i) $\nabla \cdot \bar{\mathbf{u}} \equiv 0$ and $\nabla \cdot \bar{\mathbf{u}}_b \equiv 0$,
- (ii) $\text{supp } \bar{\mathbf{u}} \cup \text{supp } \bar{\xi} \subseteq (-1/3, 1/3) \times (-1/3, 1/3) \times \mathbb{R}$,
- (iii) $\text{supp } \bar{\mathbf{u}}_b \cup \text{supp } \bar{\xi}_b \subseteq (-1/3, 1/3) \times (-1/3, 1/3) \times (-\infty, 1/4)$,
- (iv) $\bar{\mathbf{u}} \cdot \nabla \bar{\xi} \equiv 0$, while $\text{supp}_z(\bar{\mathbf{u}}_b \cdot \nabla \bar{\xi}_b) \subseteq (1/32, 5/64)$,
- (v) $\int_{\mathbb{R}^2} \int_{z=0}^{1/4} \bar{\mathbf{u}}_z \bar{\xi} \, d\mathbf{x} \geq c_3 > 0$ and $\int_{\mathbb{R}^2} \int_{z=0}^{1/8} \bar{\mathbf{u}}_{b,z} \bar{\xi}_b \, d\mathbf{x} \geq 0$.

Here, c_3 is a positive constant independent of any parameter. Furthermore, the velocity fields $\tilde{\mathbf{u}}, \tilde{\mathbf{u}}_b, \tilde{\mathbf{u}}_r$ as defined in (4.23) and the scalar fields $\tilde{\xi}, \tilde{\xi}_b, \tilde{\xi}_r$ defined in (4.30), respectively belong to $C^\infty(\mathbb{R}^3, \mathbb{R}^3)$ and $C^\infty(\mathbb{R}^3)$.

Proof of Proposition 4.2. We already proved all the points except (iv) and (v), which we prove now.

We first focus on point (iv). We note that: (1) $\text{supp } \bar{\mathbf{u}} = \text{supp } \bar{\mathbf{u}}^u \cup \text{supp } \bar{\mathbf{u}}^d$, (2) $\text{supp } \bar{\mathbf{u}}^u \subseteq S^{u, \gamma} \subset S^{u, \frac{\lambda-\gamma}{2}}$, (3) $\text{supp } \bar{\mathbf{u}}^d \subseteq S^{d, \gamma} \subset S^{d, \frac{\lambda-\gamma}{2}}$. Furthermore, because of our choices of δ, γ and λ , we see that $S^{u, \frac{\lambda-\gamma}{2}} \cap S^{d, \frac{\lambda-\gamma}{2}} = \emptyset$. Now, if $\mathbf{x} \notin S^{u, \frac{\lambda-\gamma}{2}} \cup S^{d, \frac{\lambda-\gamma}{2}}$, it clear that $(\bar{\mathbf{u}} \cdot \nabla \bar{\xi})(\mathbf{x}) = 0$, as for this case $\mathbf{x} \notin \text{supp } \bar{\mathbf{u}}$. In the next case, when $\mathbf{x} \in S^{u, \frac{\lambda-\gamma}{2}}$, we have $\bar{\xi} \equiv 1$ which implies $(\bar{\mathbf{u}} \cdot \nabla \bar{\xi})(\mathbf{x}) = 0$. In a similar manner, one can show $(\bar{\mathbf{u}} \cdot \nabla \bar{\xi})(\mathbf{x}) = 0$ when $\mathbf{x} \in S^{d, \frac{\lambda-\gamma}{2}}$.

Next, we show that $\text{supp}_z \bar{\mathbf{u}}_b \cdot \nabla \bar{\xi}_b \subseteq (1/32, 5/64)$. We first note that

$$\{z < h\} \cap \text{supp } \bar{\mathbf{u}}_b \subset \tilde{S}_b^{u, \lambda-\gamma} \cup \tilde{S}_b^{d, \lambda-\gamma},$$

and that $\tilde{S}_b^{u, \lambda-\gamma} \cap \tilde{S}_b^{d, \lambda-\gamma} = \emptyset$. For $z < h$, we proceed as in the last paragraph to show $(\bar{\mathbf{u}}_b \cdot \nabla \bar{\xi}_b)(\mathbf{x}) = 0$. When

$z > h + \lambda + \gamma$, from the definition of \tilde{S}_b^u and \tilde{S}_u^d , we see that $\bar{\xi}_b \equiv 0$, therefore, $(\bar{\mathbf{u}}_b \cdot \nabla \bar{\xi}_b)(\mathbf{x}) = 0$ in this region as well. To summarize, $\text{supp}_z \bar{\mathbf{u}}_b \cdot \nabla \bar{\xi}_b \subseteq [h, h + \gamma + \lambda] \in (1/32, 5/64)$.

Now we move to point (v) of Proposition 4.2. From a straightforward calculation, we see that

$$\begin{aligned}
\int_{\mathbb{R}^3 \cap \{0 < z < 1/4\}} \bar{u}_z \bar{\xi} d\mathbf{x} &= \int_{(\text{supp } \bar{\mathbf{u}}^u \cup \text{supp } \bar{\mathbf{u}}^d) \cap \{0 < z < 1/4\}} \bar{u}_z \bar{\xi} d\mathbf{x} \\
&= \int_{\text{supp } \bar{\mathbf{u}}^u \cap \{0 < z < 1/4\}} \bar{u}_z \bar{\xi} d\mathbf{x} + \int_{\text{supp } \bar{\mathbf{u}}^d \cap \{0 < z < 1/4\}} \bar{u}_z \bar{\xi} d\mathbf{x} \\
&= \int_{\text{supp } \bar{\mathbf{u}}^u \cap \{0 < z < 1/4\}} \bar{u}_z^u \bar{\xi} d\mathbf{x} + \int_{\text{supp } \bar{\mathbf{u}}^d \cap \{0 < z < 1/4\}} \bar{u}_z^d \bar{\xi} d\mathbf{x} \\
&= \int_{\text{supp } \bar{\mathbf{u}}^u \cap \{0 < z < 1/4\}} \bar{u}_z^u d\mathbf{x} - \int_{\text{supp } \bar{\mathbf{u}}^d \cap \{0 < z < 1/4\}} \bar{u}_z^d d\mathbf{x} \\
&= \int_{\mathbb{R}^3 \cap \{0 < z < 1/4\}} \bar{u}_z^u d\mathbf{x} - \int_{\mathbb{R}^3 \cap \{0 < z < 1/4\}} \bar{u}_z^d d\mathbf{x} \\
&= \frac{1}{4} \int_{\mathbb{R}^2} \bar{u}_z^u(\cdot, 0) dx dy - \frac{1}{4} \int_{\mathbb{R}^2} \bar{u}_z^d(\cdot, 0) dx dy \\
&= c_3 > 0,
\end{aligned} \tag{4.31}$$

where c_3 is some constant. To obtain the fourth line, we used the fact that $\xi(\mathbf{x}) = 1$ when $\mathbf{x} \in \text{supp } \bar{\mathbf{u}}^u$ and $\xi(\mathbf{x}) = -1$ when $\mathbf{x} \in \text{supp } \bar{\mathbf{u}}^d$. To obtain the sixth line, we used the fact that $\bar{\mathbf{u}}^u$ and $\bar{\mathbf{u}}^d$ are divergence-free and that their support is bounded in the xy -plane, which in turn implies that the volume flux through any horizontal section is the same, i.e.,

$$\int_{\mathbb{R}^2} \bar{u}_z^u(\cdot, z) dx dy = \int_{\mathbb{R}^2} \bar{u}_z^u(\cdot, 0) dx dy \quad \text{and} \quad \int_{\mathbb{R}^2} \bar{u}_z^d(\cdot, z) dx dy = \int_{\mathbb{R}^2} \bar{u}_z^d(\cdot, 0) dx dy \quad \text{for any } z.$$

To show

$$\int_{\mathbb{R}^3 \cap \{0 < z < 1/4\}} \bar{u}_{b,z} \bar{\xi}_b d\mathbf{x} \geq 0,$$

we simply note that $\bar{\xi}_b \equiv 0$ when $z \geq h + \lambda + \gamma$ and for $z < h + \lambda + \gamma$, the velocity $\bar{\mathbf{u}}_b$ is unidirectional (only the z -component is non-zero). Furthermore, in this region, wherever $\bar{u}_{b,z} > 0$, we have $\bar{\xi}_b \geq 0$ and wherever $\bar{u}_{b,z} < 0$, we have $\bar{\xi}_b \leq 0$. \square

4.3 Main copies $\bar{\mathbf{u}}_N$ and $\bar{\xi}_N$: Proof of Proposition 3.1

Let's begin with a few useful definitions. First, let

$$z_i := \frac{1}{2} - \frac{1}{2^{i+1}} \quad \text{for } i \in \mathbb{Z}_{\geq 0},$$

mark the vertical positions of the interfaces of different layers, while the intervals

$$Z_i := [z_{i-1}, z_i) \quad \text{for } i \in \mathbb{N}, \tag{4.32}$$

denote the different layers. We define the set

$$F := \{(1, 0), (-1, 0), (0, 1), (0, -1)\}$$

which we use to define sets of nodal points as

$$\mathcal{N}_i = \left\{ (x, y, z_i) \left| x = \sum_{j=1}^{|i|} \frac{\alpha_j}{2^{j+1}}, y = \sum_{j=1}^{|i|} \frac{\beta_j}{2^{j+1}}, (\alpha_j, \beta_j) \in F \right. \right\} \quad \text{for } i \in \mathbb{N}. \quad (4.33)$$

Proof of Proposition 3.1. For a given integer $N \geq 1$, we need to construct a velocity field $\bar{\mathbf{u}}_N$ and a scalar field $\bar{\xi}_N$ in the domain D such that they satisfy the properties specified in Proposition 3.1. To that end, we start by creating an intermediate flow field $\bar{\mathbf{u}}_{int,1} : \mathbb{R}^3 \rightarrow \mathbb{R}^3$, whose support lies in $z \geq 0$ and is defined as follows:

$$\bar{\mathbf{u}}_{int,1}(\mathbf{x}) := \bar{\mathbf{u}}(\mathbf{x}) \mathbf{1}_{Z_1} + \sum_{i=1}^{N-1} \sum_{\mathbf{p} \in \mathcal{N}_i} T^{\mathbf{p}}(\bar{\mathbf{u}}(2^i \mathbf{x})) \mathbf{1}_{Z_{i+1}} + \sum_{\mathbf{p} \in \mathcal{N}_N} T^{\mathbf{p}}(\bar{\mathbf{u}}_b(2^N \mathbf{x})) \mathbf{1}_{Z_{N+1}} \quad \text{for } \mathbf{x} \in \mathbb{R}^3. \quad (4.34)$$

To create $\bar{\mathbf{u}}_N$, we glue $\bar{\mathbf{u}}_{int,1}$ and its mirror reflection about $z = 0$. Let

$$\bar{\mathbf{u}}_{int,2}(\mathbf{x}) := (-\bar{u}_{x,int,1}(x, y, -z), -\bar{u}_{y,int,1}(x, y, -z), \bar{u}_{z,int,1}(x, y, -z)) \mathbf{1}_{z < 0} \quad \text{for } \mathbf{x} \in \mathbb{R}^3. \quad (4.35)$$

Notice that the signs of x and y components are flipped to maintain the divergence-free condition. We finally define $\bar{\mathbf{u}}_N$ as

$$\bar{\mathbf{u}}_N(\mathbf{x}) := \bar{\mathbf{u}}_{int,1}(\mathbf{x}) + \bar{\mathbf{u}}_{int,2}(\mathbf{x}). \quad (4.36)$$

Note that $\text{supp } \bar{\mathbf{u}}_N \subseteq D$ and it is really the restriction of $\bar{\mathbf{u}}_N$ to D , which we continue to call $\bar{\mathbf{u}}_N$, that we use in the proof of Proposition 3.1. We then define $\bar{\xi}_N$ in a similar way. First, we define an intermediate scalar field $\bar{\xi}_{int,1} : \mathbb{R}^3 \rightarrow \mathbb{R}$ as

$$\bar{\xi}_{int,1}(\mathbf{x}) := \bar{\xi}(\mathbf{x}) \mathbf{1}_{Z_1} + \sum_{i=1}^{N-1} \sum_{\mathbf{p} \in \mathcal{N}_i} T^{\mathbf{p}}(\bar{\xi}(2^i \mathbf{x})) \mathbf{1}_{Z_{i+1}} + \sum_{\mathbf{p} \in \mathcal{N}_N} T^{\mathbf{p}}(\bar{\xi}_b(2^N \mathbf{x})) \mathbf{1}_{Z_{N+1}} \quad \text{for } \mathbf{x} \in \mathbb{R}^3,$$

and its reflection about $z = 0$ as

$$\bar{\xi}_{int,2}(\mathbf{x}) = \bar{\xi}_{int,1}(x, y, -z) \mathbf{1}_{z < 0} \quad \text{for } \mathbf{x} \in \mathbb{R}^3,$$

using which we define

$$\bar{\xi}_N(\mathbf{x}) := \bar{\xi}_{int,1}(\mathbf{x}) + \bar{\xi}_{int,2}(\mathbf{x}) \quad \text{for } \mathbf{x} \in \mathbb{R}^3. \quad (4.37)$$

As before, $\text{supp } \bar{\xi}_N \subseteq D$ and it is the restriction of $\bar{\xi}_N$ to D , which we continue to denote as $\bar{\xi}_N$, that we use in Proposition 3.1. We claim that the velocity field $\bar{\mathbf{u}}_N$ and the scalar field $\bar{\xi}_N$ defined here satisfy all the requirements stated in Proposition 3.1.

We first show that $\text{supp } \bar{\mathbf{u}}_N \subseteq (-1/2, 1/2) \times (-1/2, 1/2) \times (-z_{N+2}, z_{N+2}) \subseteq D$. It is clear from the definition of $\bar{\mathbf{u}}_N$ given in (4.36) along with (4.34), (4.35) and the definition of Z_i in (4.32) that if $\hat{\mathbf{x}} \in \text{supp } \bar{\mathbf{u}}_N$ then

$$\hat{z} \in [-z_{N+1}, z_{N+1}] \subset (-z_{N+2}, z_{N+2}). \quad (4.38)$$

Next from the statement (ii) in Proposition 4.2, we note that if $\hat{\mathbf{x}} \in \text{supp } \bar{\mathbf{u}}(2^i \mathbf{x})$ then

$$\hat{x}, \hat{y} \in \left(-\frac{1}{3 \cdot 2^i}, \frac{1}{3 \cdot 2^i} \right).$$

Also, note that if $\mathbf{p} \in \mathcal{N}_i$ for $i \in \mathbb{N}$, then

$$|p_x|, |p_y| \leq \frac{1}{2} - \frac{1}{2^{i-1}},$$

Combining these two pieces of information tells us that if $\widehat{\mathbf{x}} \in \text{supp } T^{\mathbf{p}}\overline{\mathbf{u}}(2^i \mathbf{x})$ then

$$\widehat{x}, \widehat{y} \in \left(-\frac{1}{2} + \frac{1}{3 \cdot 2^i}, \frac{1}{2} - \frac{1}{3 \cdot 2^i}\right) \subset \left(-\frac{1}{2}, \frac{1}{2}\right). \quad (4.39)$$

Finally, combining (4.38) and (4.39) with the definition (4.36) gives

$$\text{supp } \overline{\mathbf{u}}_N \subseteq (-1/2, 1/2) \times (-1/2, 1/2) \times (-z_{N+2}, z_{N+2}) \subseteq D. \quad (4.40)$$

We now show that $\overline{\mathbf{u}}_N$ is infinitely differentiable, which together with (4.40) will imply $\overline{\mathbf{u}}_N \in C_c^\infty(D; \mathbb{R}^3)$. Let's first define two sets

$$\begin{aligned} \Lambda &:= \left(\bigcup_{0 \leq i \leq N-1} (z_i, z_{i+1}) \right) \cup \left(\bigcup_{0 \leq i \leq N-1} (-z_{i+1}, -z_i) \right) \cup (z_N, 1/2) \cup (-1/2, -z_N), \\ \Gamma &:= \{z_0, z_1, -z_1, \dots, z_N, -z_N\}. \end{aligned}$$

It is easy to see from (4.34), (4.35), (4.36) and from the infinite differentiability of $\overline{\mathbf{u}}$ and $\overline{\mathbf{u}}_b$ in Proposition 4.2 that $\overline{\mathbf{u}}_N(\mathbf{x})$ is infinitely differentiable when $z \in \Lambda$. Therefore, the only thing we still need to show is that $\overline{\mathbf{u}}_N(\mathbf{x})$ is infinitely differentiable when $z \in \Gamma$, i.e., at the interfaces.

The fact $\tilde{\mathbf{u}}_r$ in Proposition 4.2 belongs to $C^\infty(\mathbb{R}^3, \mathbb{R}^3)$ and $\overline{\mathbf{u}}_N$ coincides with $\tilde{\mathbf{u}}_r$ when $z \in (-z_1, z_1)$, implies $\overline{\mathbf{u}}_N(\mathbf{x})$ is infinite differentiable when $z = z_0$. Now if \mathbf{x} is such that $z \in (z_0, z_2)$ then $\overline{\mathbf{u}}_N(\mathbf{x})$ coincides with $\tilde{\mathbf{u}}_b(\mathbf{x})$ when $N = 1$ or it coincides with $\tilde{\mathbf{u}}(\mathbf{x})$ when $N > 1$, which then concludes the infinite differentiability of $\overline{\mathbf{u}}_N$ at $z = z_1$. A similar argument can be applied to conclude the infinite differentiability at $z = -z_1$. In the last case, when $N > 1$ and $i \in \{2, \dots, N-1\}$, then one can show

$$\begin{aligned} \overline{\mathbf{u}}_N(\mathbf{x}) &= \sum_{\mathbf{p} \in \mathcal{N}_{i-1}} T^{\mathbf{p}}(\overline{\mathbf{u}}(2^{i-1} \mathbf{x})) \mathbf{1}_{Z_i} + \sum_{\mathbf{p} \in \mathcal{N}_i} T^{\mathbf{p}}(\overline{\mathbf{u}}(2^i \mathbf{x})) \mathbf{1}_{Z_{i+1}} \\ &= \sum_{\mathbf{p} \in \mathcal{N}_{i-1}} T^{\mathbf{p}} \left(\left(\overline{\mathbf{u}} + \sum_{\mathbf{p}' \in \mathcal{N}_1} T^{\mathbf{p}'} \overline{\mathbf{u}} \right) (2^{i-1} \mathbf{x}) \right) \\ &= \sum_{\mathbf{p} \in \mathcal{N}_{i-1}} T^{\mathbf{p}}(\tilde{\mathbf{u}}(2^{i-1} \mathbf{x})) \quad \text{when } \mathbf{x} \in (z_{i-1}, z_{i+1}), \end{aligned}$$

or when $i = N$, then

$$\overline{\mathbf{u}}_N(\mathbf{x}) = \sum_{\mathbf{p} \in \mathcal{N}_{i-1}} T^{\mathbf{p}}(\tilde{\mathbf{u}}_b(2^{i-1} \mathbf{x})) \quad \text{when } \mathbf{x} \in (z_{i-1}, z_{i+1}),$$

which then establishes that $\overline{\mathbf{u}}_N(\mathbf{x})$ is infinitely differentiable when $z = z_i$ for $2 \leq i \leq N$. A similar argument applies when $z = -z_i$ for $2 \leq i \leq N$, which finishes the proof of $\overline{\mathbf{u}}_N \in C_c^\infty(D; \mathbb{R}^3)$. We note similar arguments will also work to show $\bar{\xi}_N \in C_c^\infty(D)$.

It is now fairly easy prove (i) in Proposition 3.1. It is trivial to see that $\nabla \cdot \overline{\mathbf{u}}_N = 0$ when $z \in \Lambda$. As $\overline{\mathbf{u}}_N \in C_c^\infty(D; \mathbb{R}^3)$, the derivatives of $\overline{\mathbf{u}}_N$ are continuous in D , which leads us to conclude that $\nabla \cdot \overline{\mathbf{u}}_N = 0$ everywhere in D .

Next, we see that (4.40) and a similar conclusion derived for $\bar{\xi}_N$ proves (ii) in Proposition 3.1.

To prove (iii) in Proposition 3.1, we need the following simple lemma.

Lemma 4.5. For $i \in \mathbb{N}$, let $\mathbf{p}_1, \mathbf{p}_2 \in \mathcal{N}_i$ such that $\mathbf{p}_1 \neq \mathbf{p}_2$, then

$$\begin{aligned} &(\text{supp } T^{\mathbf{p}_1} \overline{\mathbf{u}}(2^i \mathbf{x}) \cup \text{supp } T^{\mathbf{p}_1} \bar{\xi}(2^i \mathbf{x})) \cap (\text{supp } T^{\mathbf{p}_2} \overline{\mathbf{u}}(2^i \mathbf{x}) \cup \text{supp } T^{\mathbf{p}_2} \bar{\xi}(2^i \mathbf{x})) = \emptyset, \\ &(\text{supp } T^{\mathbf{p}_1} \overline{\mathbf{u}}_b(2^i \mathbf{x}) \cup \text{supp } T^{\mathbf{p}_1} \bar{\xi}_b(2^i \mathbf{x})) \cap (\text{supp } T^{\mathbf{p}_2} \overline{\mathbf{u}}_b(2^i \mathbf{x}) \cup \text{supp } T^{\mathbf{p}_2} \bar{\xi}_b(2^i \mathbf{x})) = \emptyset. \end{aligned}$$

Proof of Lemma 4.5. As $\mathbf{p}_1 \neq \mathbf{p}_2$, from the definition (4.33) of \mathcal{N}_i , we note the following lower bound on the absolute difference of x and y coordinates of \mathbf{p}_1 and \mathbf{p}_2 :

$$|\mathbf{p}_{1,x} - \mathbf{p}_{2,x}| \geq \frac{1}{2^i} \quad \text{and} \quad |\mathbf{p}_{1,y} - \mathbf{p}_{2,y}| \geq \frac{1}{2^i},$$

which implies

$$|\mathbf{p}_1 - \mathbf{p}_2|_{\parallel} \geq \frac{\sqrt{2}}{2^i}.$$

Now, if $\mathbf{x}_1 \in (\text{supp } T^{\mathbf{p}_1} \bar{\mathbf{u}}(2^i \mathbf{x}) \cup \text{supp } T^{\mathbf{p}_1} \bar{\xi}(2^i \mathbf{x}))$ or $\mathbf{x}_1 \in (\text{supp } T^{\mathbf{p}_1} \bar{\mathbf{u}}_b(2^i \mathbf{x}) \cup \text{supp } T^{\mathbf{p}_1} \bar{\xi}_b(2^i \mathbf{x}))$ and if $\mathbf{x}_2 \in (\text{supp } T^{\mathbf{p}_2} \bar{\mathbf{u}}(2^i \mathbf{x}) \cup \text{supp } T^{\mathbf{p}_2} \bar{\xi}(2^i \mathbf{x}))$ or $\mathbf{x}_2 \in (\text{supp } T^{\mathbf{p}_2} \bar{\mathbf{u}}_b(2^i \mathbf{x}) \cup \text{supp } T^{\mathbf{p}_2} \bar{\xi}_b(2^i \mathbf{x}))$, then using the statements (ii) and (iii) from Proposition 4.2, we see that

$$|\mathbf{x}_1 - \mathbf{p}_1|_{\parallel} \leq \frac{\sqrt{2}}{3 \cdot 2^i} \quad \text{and} \quad |\mathbf{x}_2 - \mathbf{p}_2|_{\parallel} \leq \frac{\sqrt{2}}{3 \cdot 2^i}.$$

We can now finish the proof with a simple application of the triangle inequality as

$$|\mathbf{x}_1 - \mathbf{x}_2| \geq |\mathbf{p}_1 - \mathbf{p}_2|_{\parallel} - |\mathbf{x}_1 - \mathbf{p}_1|_{\parallel} - |\mathbf{x}_2 - \mathbf{p}_2|_{\parallel} \geq \frac{\sqrt{2}}{3 \cdot 2^i}.$$

□

Using the lemma, we can write

$$\begin{aligned} (\bar{\mathbf{u}}_{int,1} \cdot \nabla \bar{\xi}_{int,1})(\mathbf{x}) &= \bar{\mathbf{u}}(\mathbf{x}) \cdot \nabla \bar{\xi}(\mathbf{x}) \mathbf{1}_{Z_1} + \sum_{i=1}^{N-1} \sum_{\mathbf{p} \in \mathcal{N}_i} T^{\mathbf{p}}(\bar{\mathbf{u}}(2^i \mathbf{x})) \cdot \nabla T^{\mathbf{p}}(\bar{\xi}(2^i \mathbf{x})) \mathbf{1}_{Z_{i+1}} \\ &\quad + \sum_{\mathbf{p} \in \mathcal{N}_N} T^{\mathbf{p}}(\bar{\mathbf{u}}_b(2^N \mathbf{x})) \cdot \nabla T^{\mathbf{p}}(\bar{\xi}_b(2^N \mathbf{x})) \mathbf{1}_{Z_{N+1}} \quad \text{for } z \in \Lambda, \end{aligned}$$

which implies

$$\begin{aligned} (\bar{\mathbf{u}}_{int,1} \cdot \nabla \bar{\xi}_{int,1})(\mathbf{x}) &= \bar{\mathbf{u}}(\mathbf{x}) \cdot \nabla \bar{\xi}(\mathbf{x}) \mathbf{1}_{Z_1} + \sum_{i=1}^{N-1} \sum_{\mathbf{p} \in \mathcal{N}_i} T^{\mathbf{p}}(\bar{\mathbf{u}}(2^i \mathbf{x}) \cdot \nabla \bar{\xi}(2^i \mathbf{x})) \mathbf{1}_{Z_{i+1}} \\ &\quad + \sum_{\mathbf{p} \in \mathcal{N}_N} T^{\mathbf{p}}(\bar{\mathbf{u}}_b(2^N \mathbf{x}) \cdot \nabla \bar{\xi}_b(2^N \mathbf{x})) \mathbf{1}_{Z_{N+1}} \quad \text{for } z \in \Lambda. \end{aligned} \quad (4.42)$$

Using (4.42) and point (iv) from Proposition 4.2, we conclude

$$(\bar{\mathbf{u}}_{int,1} \cdot \nabla \bar{\xi}_{int,1})(\mathbf{x}) = 0 \quad \text{when } z \in \Lambda \setminus \left(\frac{1}{2} - \frac{15}{32 \cdot 2^N}, \frac{1}{2} - \frac{27}{64 \cdot 2^N} \right) \quad (4.43)$$

A simple calculation then shows that

$$(\bar{\mathbf{u}}_N \cdot \nabla \bar{\xi}_N)(x, y, z) = -(\bar{\mathbf{u}}_N \cdot \nabla \bar{\xi}_N)(x, y, -z) \quad \text{when } z \in \Lambda \quad (4.44)$$

which, combined with the result (4.43) and the fact that $\bar{\mathbf{u}}_N$ and the derivatives of $\bar{\xi}_N$ are continuous when $z \in \Gamma$, help us conclude

$$(\bar{\mathbf{u}}_N \cdot \nabla \bar{\xi}_N)(\mathbf{x}) = 0 \quad \text{when } \mathbf{x} \in \Gamma.$$

In total, we then have

$$\text{supp}_z(\bar{\mathbf{u}}_N \cdot \nabla \bar{\xi}_N) \subseteq \left(\frac{1}{2} - \frac{15}{32 \cdot 2^N}, \frac{1}{2} - \frac{27}{64 \cdot 2^N} \right) \cup \left(-\frac{1}{2} + \frac{27}{64 \cdot 2^N}, -\frac{1}{2} + \frac{15}{32 \cdot 2^N} \right).$$

To prove (iv) in Proposition 3.1, we note from (4.42) and point (iv) in Proposition 4.2 that

$$(\bar{\mathbf{u}}_{int,1} \cdot \nabla \bar{\xi}_{int,1})(\mathbf{x}) = \sum_{\mathbf{p} \in \mathcal{N}_N} 2^N T^{\mathbf{p}}((\bar{\mathbf{u}}_b \cdot \nabla \bar{\xi}_b)(2^N \mathbf{x})) \mathbf{1}_{Z_{N+1}} \quad \text{for } z \in \Lambda,$$

which when combined with Lemma 4.5, implies

$$\|\bar{\mathbf{u}}_{int,1} \cdot \nabla \bar{\xi}_{int,1}\|_{L^\infty(D)} \leq 2^N \|\bar{\mathbf{u}}_b \cdot \nabla \bar{\xi}_b\|_{L^\infty(\mathbb{R}^3)}.$$

Noting (4.44) and that $\bar{\mathbf{u}}_N \cdot \nabla \bar{\xi}_N$ coincides with $\bar{\mathbf{u}}_{int,1} \cdot \nabla \bar{\xi}_{int,1}$ when $z > 0$, we have

$$\|\bar{\mathbf{u}}_N \cdot \nabla \bar{\xi}_N\|_{L^\infty(D)} \leq 2^N \|\bar{\mathbf{u}}_b \cdot \nabla \bar{\xi}_b\|_{L^\infty(\mathbb{R}^3)}.$$

Now $\bar{\mathbf{u}}_b \cdot \nabla \bar{\xi}_b$ is an infinite differentiable function and its support lies in a bounded set from (iii) and (iv) in Proposition 4.2, therefore $\|\bar{\mathbf{u}}_b \cdot \nabla \bar{\xi}_b\|_{L^\infty(\mathbb{R}^3)}$ is bounded and we can conclude that

$$\|\bar{\mathbf{u}}_N \cdot \nabla \bar{\xi}_N\|_{L^\infty(D)} \lesssim 2^N.$$

Proof of (v) in Proposition 3.1 is a simple computation. Once again using Lemma 4.5, one can write the following

$$\begin{aligned} \int_D |\nabla \bar{\mathbf{u}}_N|^2 d\mathbf{x} &= 2 \int_{\{0 < z < 1/2\}} |\nabla \bar{\mathbf{u}}_{int,1}|^2 d\mathbf{x} \\ &= 2 \int_{\{z \in Z_1\}} |\nabla \bar{\mathbf{u}}(\mathbf{x})|^2 d\mathbf{x} + 2 \sum_{i=1}^{N-1} \sum_{\mathbf{p} \in \mathcal{N}_i} \int_{\{z \in Z_{i+1}\}} |\nabla T^{\mathbf{p}}(\bar{\mathbf{u}}(2^i \mathbf{x}))|^2 d\mathbf{x} \\ &\quad + 2 \sum_{\mathbf{p} \in \mathcal{N}_N} \int_{\{z \in Z_{N+1}\}} |\nabla T^{\mathbf{p}}(\bar{\mathbf{u}}_b(2^N \mathbf{x}))|^2 d\mathbf{x}. \end{aligned}$$

After an appropriate translation and dilation of the coordinate variables and noting that $|\mathcal{N}_i| = 4^i$, one can show that

$$\begin{aligned} \int_D |\nabla \bar{\mathbf{u}}_N|^2 d\mathbf{x} &= \left(\sum_{i=0}^{N-1} 2^{i+1} \right) \int_{Z_1} |\nabla \bar{\mathbf{u}}(\mathbf{x})|^2 d\mathbf{x} + 2^{N+1} \int_{\{z \in Z_1\}} |\nabla \bar{\mathbf{u}}_b(\mathbf{x})|^2 d\mathbf{x} \\ &= 2^{N+1} \max \left\{ \int_{\{z \in Z_1\}} |\nabla \bar{\mathbf{u}}(\mathbf{x})|^2 d\mathbf{x}, \int_{\{z \in Z_1\}} |\nabla \bar{\mathbf{u}}_b(\mathbf{x})|^2 d\mathbf{x} \right\} \lesssim 2^N. \end{aligned}$$

Similarly, one can also conclude

$$\int_D |\nabla \bar{\xi}_N|^2 d\mathbf{x} \lesssim 2^N,$$

which then proves (v).

The proof of (vi) in Proposition 3.1 is also very similar to that of (v). We first write

$$\begin{aligned} \int_D \bar{u}_{N,z} \bar{\xi}_N \, d\mathbf{x} &= 2 \int_{\{0 < z < 1/2\}} \bar{u}_{int,1,z} \bar{\xi}_{int,1} \, d\mathbf{x} \\ &= 2 \int_{\{z \in Z_1\}} \bar{u}_z \bar{\xi} \, d\mathbf{x} + 2 \sum_{i=1}^{N-1} \sum_{\mathbf{p} \in \mathcal{N}_i} \int_{\{z \in Z_{i+1}\}} T^{\mathbf{p}}(\bar{u}_z(2^i \mathbf{x})) T^{\mathbf{p}}(\bar{\xi}(2^i \mathbf{x})) \, d\mathbf{x} \\ &\quad + 2 \sum_{\mathbf{p} \in \mathcal{N}_N} \int_{\{z \in Z_{N+1}\}} T^{\mathbf{p}}(\bar{u}_{b,z}(2^i \mathbf{x})) T^{\mathbf{p}}(\bar{\xi}_b(2^i \mathbf{x})) \, d\mathbf{x}. \end{aligned}$$

After an appropriate translation and dilation of the coordinate variables and noting that $|\mathcal{N}_i| = 4^i$, we obtain

$$\int_D \bar{u}_{N,z} \bar{\xi}_N \, d\mathbf{x} = \left(\sum_{i=0}^{N-1} 2^{-i+1} \right) \int_{\{z \in Z_1\}} \bar{u}_z \bar{\xi} \, d\mathbf{x} + 2^{-N+1} \int_{\{z \in Z_1\}} \bar{u}_{b,z} \bar{\xi}_b \, d\mathbf{x} \geq 2c_3 > 0,$$

where c_3 is a strictly positive constant independent of N . \square

5 A useful estimate for the solution of the Poisson's equation: Proof of Proposition 3.2

The aim of this section is to give an estimate on the solution of Poisson's equation $\Delta\varphi = f$ solved between parallel boundaries with homogeneous Dirichlet boundary conditions imposed on φ . In particular, we are interested in obtaining bounds on the L^2 norm of $\nabla\varphi$ for a given specific form of the function f . The calculations done in this section will be helpful in establishing an upper bound on the nonlocal term $\int_{\Omega} |\nabla\Delta^{-1} \operatorname{div}(\mathbf{u}\xi)|^2$ from the section 3 (see calculation (3.7)). The basic idea is to write down the solution of Poisson's equation using the Green's function method and then obtain estimates on the derivative of the Green's function to achieve our goal.

The domain of interest for this section is

$$D := \mathbb{R} \times \mathbb{R} \times (-1/2, 1/2),$$

as defined in section 2 with boundary

$$\partial D := \partial D_+ \cup \partial D_- := \mathbb{R} \times \mathbb{R} \times \{1/2\} \cup \mathbb{R} \times \mathbb{R} \times \{-1/2\}.$$

Now, suppose φ solves Poisson's equation

$$\Delta\varphi = f \quad \text{in } D, \tag{5.1}$$

with boundary condition

$$\varphi = 0 \quad \text{on } \partial D. \tag{5.2}$$

Then for a sufficiently smooth function f , we can write the solution of Poisson's equation using a Green's function

$$\varphi(\mathbf{x}) = \int_D G(\mathbf{x}, \mathbf{x}') f(\mathbf{x}') \, d\mathbf{x}, \tag{5.3}$$

where $G : D \times D \rightarrow [-\infty, \infty]$ is given by

$$G(\mathbf{x}, \mathbf{x}') := K(|\mathbf{x} - \mathbf{x}'|, z, z') \tag{5.4}$$

and

$$K(\sigma, z, z') := \int_1^\infty I(\sigma, z, z', \tau) \frac{d\tau}{\sqrt{\tau^2 - 1}}, \quad (5.5)$$

$$I(\sigma, z, z', \tau) := \frac{\cos(\pi z) \cos(\pi z') \sinh(\pi \tau \sigma)}{2\pi [\cosh(\pi \tau \sigma) + \cos \pi(z' + z)] [\cosh(\pi \tau \sigma) - \cos \pi(z' - z)]}. \quad (5.6)$$

In particular, we have the following theorem

Theorem 5.1 (Solution of the Poisson's equation). *Let $f \in C^2(D) \cap L^\infty(D)$ whose support lies a finite distance away from the boundary, i.e., $\text{supp } f \subseteq \mathbb{R} \times \mathbb{R} \times (-1/2 + \beta, 1/2 - \beta)$ for some $\beta \in (0, 1/2)$. Then φ given by (5.3) belongs to $C^2(D)$ and solves the Poisson's equation (5.1) with boundary condition (5.2).*

Proof. The proof of the theorem is a standard one and is therefore omitted from the paper. The proof relies on the method of images to write the desired Green's function between parallel boundaries as a sum of appropriately translated Green's functions corresponding to the whole space \mathbb{R}^3 , where the summation is then performed using Cauchy's residue theorem. \square

Once we know that the solution φ of the Poisson's equation is given by (5.3), we can use it to calculate $\nabla \varphi$. If $f \in L^\infty(D)$ then by an application of the mean value theorem and the dominated convergence theorem, we can perform differentiation under the integral sign in (5.3), which leads to

$$\nabla \varphi = \int_D \nabla_{\mathbf{x}} G(\mathbf{x}, \mathbf{x}') f(\mathbf{x}') d\mathbf{x}. \quad (5.7)$$

From (5.7), we see that estimates on $\nabla_{\mathbf{x}} G(\mathbf{x}, \mathbf{x}')$ can provide an upper bound on $|\nabla \varphi|$. Next, we state our result in that direction, but first, we note the following.

For clarity, we use a and b as placeholders for

$$\left| \frac{2}{\pi} \sin \left(\frac{\pi(z - z')}{2} \right) \right| \quad \text{and} \quad \left| \frac{2}{\pi} \cos \left(\frac{\pi(z + z')}{2} \right) \right| \quad (5.8)$$

respectively in the rest of this section and we will use the fact that

$$b^2 - a^2 = \frac{4}{\pi^2} \cos \pi z \cos \pi z' \geq 0 \quad \text{when} \quad z, z' \in (-1/2, 1/2) \quad (5.9)$$

in several places. We will use c for a positive constant (not necessarily the same in all places) independent of any parameters.

Proposition 5.2. *Let $f \in L^\infty(D)$ and let φ be defined by the formula (5.3), then the following holds:*

$$|\nabla \varphi|(\mathbf{x}) \leq \|f\|_{L^\infty(D)} \int_{\text{supp}_z f} g(z, z') dz'$$

where

$$g(z, z') = c \left(\log \left(1 + \frac{(b^2 - a^2)}{a^2} \right) + \frac{\cos \pi z'}{b} \right) \quad (5.10)$$

and $c > 0$ is a positive constant.

The functions f that are of special interests to us are those which are supported in a “thin layers” close to the boundaries. From Proposition 5.2, we can derive the following result for such functions.

Corollary 5.3. *Let $f \in L^\infty(D)$ such that $\text{supp } f \subseteq \mathbb{R} \times \mathbb{R} \times (1/2 - c_1 \varepsilon, 1/2 - c_2 \varepsilon) \cup \mathbb{R} \times \mathbb{R} \times (-1/2 + c_2 \varepsilon, -1/2 + c_1 \varepsilon)$, where $0 < c_2 < c_1 < 1$ and $\varepsilon < 1/4$ are three constants. If φ is defined by the formula (5.3), then the following*

holds

$$\frac{1}{l_x l_y} \int_{-l_x/2}^{l_x/2} \int_{-l_y/2}^{l_y/2} \int_{-1/2}^{1/2} |\nabla \varphi|^2 dz dy dx \lesssim \varepsilon^3 \|f\|_{L^\infty(D)}^2. \quad (5.11)$$

Proof of Proposition 3.2. We identify a $l_x - l_y$ -periodic function on D with the function f . Then using Corollary 5.3, we can finish the proof. \square

Proof of Corollary 5.3. We note from Proposition 5.2

$$\begin{aligned} & \frac{1}{l_x l_y} \int_{-l_y/2}^{l_y/2} \int_{-l_x/2}^{l_x/2} \int_{-1/2}^{1/2} |\nabla \varphi|^2 dz dx dy \leq \|f\|_{L^\infty(D)}^2 \int_{-1/2}^{1/2} \left(\int_{\text{supp}_z f} g(z, z') dz' \right)^2 dz \\ & = \|f\|_{L^\infty(D)}^2 \int_0^{1/2} \left(\int_{\text{supp}_z f} g(z, z') dz' \right)^2 dz + \|f\|_{L^\infty(D)}^2 \int_{-1/2}^0 \left(\int_{\text{supp}_z f} g(z, z') dz' \right)^2 dz. \end{aligned} \quad (5.12)$$

We focus on obtaining a bound on the first term (where the integral is carried from $z = 0$ to $z = 1/2$) in (5.12), as the calculation for the other integral is identical.

When $z' \in (1/2 - c_1\varepsilon, 1/2 - c_2\varepsilon) \cup (-1/2 + c_2\varepsilon, -1/2 + c_1\varepsilon)$ and $z \geq 0$, the following simple succession of inequalities hold:

$$b \geq \frac{1}{\pi} \max\{\cos \pi z, \cos \pi z'\} \quad (5.13a)$$

$$b \geq \frac{1}{2\pi} (\cos \pi z + \cos \pi z') \geq \frac{1}{4} \left(\frac{1}{2} - z + c_2\varepsilon \right) \quad (5.13b)$$

$$\frac{\pi c_2\varepsilon}{2} \leq \cos \pi z' \leq \pi c_1\varepsilon \quad (5.13c)$$

$$\frac{\pi}{4} - \frac{\pi z}{2} \leq \cos \pi z \leq \frac{\pi}{2} - \pi z \quad (5.13d)$$

$$a \geq \frac{1}{2} \left(\frac{1}{2} - c_1\varepsilon - z \right) \quad \text{when} \quad \frac{1}{2} - 2c_1\varepsilon \geq z \geq 0 \quad (5.13e)$$

$$a \geq \frac{1}{2} |z - z'| \quad \text{when} \quad \frac{1}{2} \geq z \geq \frac{1}{2} - 2c_1\varepsilon \quad (5.13f)$$

$$a \geq \frac{1}{5} \quad \text{when} \quad z' \in (-1/2 + c_2\varepsilon, -1/2 + c_1\varepsilon) \quad (5.13g)$$

$$\log(1 + \alpha) \leq \alpha \quad \text{when} \quad \alpha \geq 0 \quad (5.13h)$$

Here, (5.13c), (5.13d), (5.13e) and (5.13f) are a simple consequence of the inequality $z/2 \leq \sin z \leq z$ when $z \in [0, \pi/2]$, whereas (5.13a) is obtained by simple applications of trigonometric identities and (5.13b) is a result of (5.13a), (5.13c) and (5.13d). The result (5.13g) is a consequence of the assumption $0 < c_2 < c_1 < 1$. Finally, (5.13h) can be derived using a Taylor series expansion.

Next, using (5.10) and the Young's inequality, we can write

$$\begin{aligned} & \left(\int_{\text{supp}_z f} g(z, z') dz' \right)^2 \lesssim \left(\int_{\text{supp}_z f \cap \mathbb{R}_+} \log \left(1 + \frac{(b^2 - a^2)}{a^2} \right) dz' \right)^2 \\ & + \left(\int_{\text{supp}_z f \cap \mathbb{R}_-} \log \left(1 + \frac{(b^2 - a^2)}{a^2} \right) dz' \right)^2 + \left(\int_{\text{supp}_z f} \frac{\cos \pi z'}{b} dz' \right)^2 \end{aligned} \quad (5.14)$$

Using (5.13b) and (5.13c), the last term in (5.14) can be bounded from above by

$$\lesssim \frac{\varepsilon^4}{\left(\frac{1}{2} - z + c_2\varepsilon\right)^2}, \quad (5.15)$$

Using (5.9), (5.13c), (5.13g) and (5.13h), the second term in (5.14) satisfies the bound

$$\lesssim \varepsilon^4. \quad (5.16)$$

We divide the calculation of the first term in (5.14) into two cases, when $0 \leq z \leq 1/2 - 2c_1\varepsilon$ and when $1/2 - 2c_1\varepsilon \leq z \leq 1/2$. In the first case, using (5.9), (5.13c), (5.13d), (5.13e) and (5.13h), we conclude the first term is

$$\lesssim \frac{\varepsilon^4}{\left(\frac{1}{2} - z - c_1\varepsilon\right)^2}. \quad (5.17)$$

In the second case, when $1/2 - 2c_1\varepsilon \leq z \leq 1/2$, we use (5.9), (5.13c), (5.13d), (5.13f), which gives

$$\lesssim \varepsilon^2. \quad (5.18)$$

Note that in this calculation we do not use the estimate (5.13h). After using (5.13f), we have a logarithmic singularity in the integrand but it is integrable.

Finally, collecting the results (5.15), (5.16), (5.17) and (5.18), and carrying out an integration in z from 0 to $1/2$, one can bound the first term in (5.12) as

$$\lesssim \varepsilon^3 \|f\|_{L^\infty(D)}^2.$$

A similar calculation can be performed for the second term in (5.12) and the same result can be derived which then finishes the proof. \square

5.1 Proof of Proposition 5.2

To prove Proposition 5.2, we need to obtain estimates on $\nabla_{\mathbf{x}} G(\mathbf{x}, \mathbf{x}')$. From (5.4), we notice that the derivative of $G(\mathbf{x}, \mathbf{x}')$ with respect to x can be written as

$$\frac{\partial}{\partial x} G(\mathbf{x}, \mathbf{x}') = \frac{\partial |\mathbf{x} - \mathbf{x}'|_{\parallel}}{\partial x} \cdot \frac{\partial}{\partial \sigma} K(\sigma, z, z') \Big|_{\sigma=|\mathbf{x}-\mathbf{x}'|_{\parallel}} = \frac{(x - x')}{|\mathbf{x} - \mathbf{x}'|_{\parallel}} \cdot \frac{\partial}{\partial \sigma} K(\sigma, z, z') \Big|_{\sigma=|\mathbf{x}-\mathbf{x}'|_{\parallel}},$$

which leads to the following estimate

$$\left| \frac{\partial}{\partial x} G(\mathbf{x}, \mathbf{x}') \right| \leq \left(\left| \frac{\partial}{\partial \sigma} K(\sigma, z, z') \right| \right) \Big|_{\sigma=|\mathbf{x}-\mathbf{x}'|_{\parallel}}. \quad (5.19)$$

A similar calculation for the y -derivative of $G(\mathbf{x}, \mathbf{x}')$ leads to

$$\left| \frac{\partial}{\partial y} G(\mathbf{x}, \mathbf{x}') \right| \leq \left(\left| \frac{\partial}{\partial \sigma} K(\sigma, z, z') \right| \right) \Big|_{\sigma=|\mathbf{x}-\mathbf{x}'|_{\parallel}}, \quad (5.20)$$

while the estimate for the z -derivative of $G(\mathbf{x}, \mathbf{x}')$ simply is

$$\left| \frac{\partial}{\partial z} G(\mathbf{x}, \mathbf{x}') \right| \leq \left(\left| \frac{\partial}{\partial z} K(\sigma, z, z') \right| \right) \Big|_{\sigma=|\mathbf{x}-\mathbf{x}'|_{\parallel}}. \quad (5.21)$$

Using (5.19), (5.20) and (5.21), we conclude that

$$\begin{aligned} |\nabla_{\mathbf{x}} G(\mathbf{x}, \mathbf{x}')| &\leq \left| \frac{\partial}{\partial x} G(\mathbf{x}, \mathbf{x}') \right| + \left| \frac{\partial}{\partial y} G(\mathbf{x}, \mathbf{x}') \right| + \left| \frac{\partial}{\partial z} G(\mathbf{x}, \mathbf{x}') \right| \\ &\leq 2 \left(\left| \frac{\partial}{\partial \sigma} K(\sigma, z, z') \right| \right) \Big|_{\sigma=|\mathbf{x}-\mathbf{x}'|_{\parallel}} + \left(\left| \frac{\partial}{\partial z} K(\sigma, z, z') \right| \right) \Big|_{\sigma=|\mathbf{x}-\mathbf{x}'|_{\parallel}} \leq H(|\mathbf{x} - \mathbf{x}'|_{\parallel}, z, z'), \end{aligned} \quad (5.22)$$

for some suitable $H : \mathbb{R}_+ \times (-1/2, 1/2) \times (-1/2, 1/2) \rightarrow [0, +\infty]$. It then follows that

$$\begin{aligned} |\nabla \varphi(\mathbf{x})| &\leq \|f\|_{L^\infty(D)} \int_{-\infty}^{\infty} \int_{-\infty}^{\infty} \int_{\text{supp}_z f} H(|\mathbf{x} - \mathbf{x}'|_{\parallel}, z, z') \, dz' \, dx' \, dy', \\ &= \|f\|_{L^\infty(D)} \int_{-\infty}^{\infty} \int_{-\infty}^{\infty} \int_{\text{supp}_z f} H(|\mathbf{x}'|_{\parallel}, z, z') \, dz' \, dx' \, dy'. \end{aligned}$$

By considering a transformation from Cartesian coordinates to cylindrical coordinates

$$(x', y', z') \mapsto (\sigma, \theta, z')$$

one obtains

$$\begin{aligned} |\nabla \varphi(\mathbf{x})| &\leq \|f\|_{L^\infty(D)} \int_0^{\infty} \int_0^{2\pi} \int_{\text{supp}_z f} \sigma H(\sigma, z, z') \, dz' \, d\theta \, d\sigma, \\ &\lesssim \|f\|_{L^\infty(D)} \int_0^{\infty} \int_{\text{supp}_z f} \sigma H(\sigma, z, z') \, dz' \, d\sigma. \end{aligned}$$

So, to prove Proposition 5.2, we need to find an appropriate $H(\sigma, z, z')$ and then perform the integral

$$\int_0^{\infty} \sigma H(\sigma, z, z') \, d\sigma, \quad (5.23)$$

which is our next goal.

To calculate (5.19), (5.20) and (5.21), we need the derivative of $K(\sigma, z, z')$ with σ and z . Using (5.5) and (5.6) along with an application of the mean value theorem and the dominated convergence theorem leads to

$$\frac{\partial K}{\partial \sigma} = \int_1^{\infty} I_{\sigma 1} \frac{d\tau}{\sqrt{\tau^2 - 1}} + \int_1^{\infty} I_{\sigma 2} \frac{d\tau}{\sqrt{\tau^2 - 1}} + \int_1^{\infty} I_{\sigma 3} \frac{d\tau}{\sqrt{\tau^2 - 1}}, \quad (5.24)$$

and

$$\frac{\partial K}{\partial z} = \int_1^{\infty} I_{z 1} \frac{d\tau}{\sqrt{\tau^2 - 1}} + \int_1^{\infty} I_{z 2} \frac{d\tau}{\sqrt{\tau^2 - 1}} + \int_1^{\infty} I_{z 3} \frac{d\tau}{\sqrt{\tau^2 - 1}}, \quad (5.25)$$

where

$$I_{\sigma 1} := \frac{\cos(\pi z) \cos(\pi z') \tau \cosh(\pi \tau \sigma)}{2 [\cosh(\pi \tau \sigma) + \cos \pi(z' + z)] [\cosh(\pi \tau \sigma) - \cos \pi(z' - z)]}, \quad (5.26a)$$

$$I_{\sigma 2} := -\frac{\cos(\pi z) \cos(\pi z') \tau \sinh^2(\pi \tau \sigma)}{2 [\cosh(\pi \tau \sigma) + \cos \pi(z' + z)]^2 [\cosh(\pi \tau \sigma) - \cos \pi(z' - z)]}, \quad (5.26b)$$

$$I_{\sigma 3} := -\frac{\cos(\pi z) \cos(\pi z') \tau \sinh^2(\pi \tau \sigma)}{2 [\cosh(\pi \tau \sigma) + \cos \pi(z' + z)] [\cosh(\pi \tau \sigma) - \cos \pi(z' - z)]^2}, \quad (5.26c)$$

$$I_{z 1} = -\frac{\sin(\pi z) \cos(\pi z') \sinh(\pi \tau \sigma)}{2 [\cosh(\pi \tau \sigma) + \cos \pi(z' + z)] [\cosh(\pi \tau \sigma) - \cos \pi(z' - z)]}, \quad (5.26d)$$

$$I_{z 2} = \frac{\cos(\pi z) \cos(\pi z') \sin \pi(z' + z) \sinh(\pi \tau \sigma)}{2 [\cosh(\pi \tau \sigma) + \cos \pi(z' + z)]^2 [\cosh(\pi \tau \sigma) - \cos \pi(z' - z)]}, \quad (5.26e)$$

$$I_{z 3} = \frac{\cos(\pi z) \cos(\pi z') \sin \pi(z' - z) \sinh(\pi \tau \sigma)}{2 [\cosh(\pi \tau \sigma) + \cos \pi(z' + z)] [\cosh(\pi \tau \sigma) - \cos \pi(z' - z)]^2}. \quad (5.26f)$$

Next, we state a few important lemmas to bound the derivatives of $K(\sigma, z, z')$. We will always implicitly assume that $z, z' \in (-1/2, 1/2)$.

Lemma 5.1. *Let $\sigma \geq \frac{1}{2\pi}$, then we have*

(i)

$$\int_1^\infty (|I_{\sigma 1}| + |I_{\sigma 2}| + |I_{\sigma 3}|) \frac{d\tau}{\sqrt{\tau^2 - 1}} \lesssim \cos(\pi z') \exp(-\pi \sigma).$$

(ii)

$$\int_1^\infty (|I_{z 1}| + |I_{z 2}| + |I_{z 3}|) \frac{d\tau}{\sqrt{\tau^2 - 1}} \lesssim \cos(\pi z') \exp(-\pi \sigma).$$

Lemma 5.2. *Let $0 < \sigma < \frac{1}{2\pi}$, then we have*

(i)

$$\int_{\frac{1}{\pi\sigma}}^\infty (|I_{\sigma 1}| + |I_{\sigma 2}| + |I_{\sigma 3}|) \frac{d\tau}{\sqrt{\tau^2 - 1}} \lesssim \frac{\cos(\pi z')}{\sigma}.$$

(ii)

$$\int_{\frac{1}{\pi\sigma}}^\infty (|I_{z 1}| + |I_{z 2}| + |I_{z 3}|) \frac{d\tau}{\sqrt{\tau^2 - 1}} \lesssim \cos(\pi z').$$

Lemma 5.3. *Let $0 < \sigma < \frac{1}{2\pi}$ and $z \neq z'$, then we have*

(i)

$$\int_1^{\frac{1}{\pi\sigma}} (|I_{\sigma 1}| + |I_{\sigma 2}| + |I_{\sigma 3}|) \frac{d\tau}{\sqrt{\tau^2 - 1}} \lesssim \frac{1}{\sigma} \left[\frac{1}{\sqrt{\sigma^2 + a^2}} - \frac{1}{\sqrt{\sigma^2 + b^2}} \right].$$

(ii)

$$\int_1^{\frac{1}{\pi\sigma}} |I_{z 1}| \frac{d\tau}{\sqrt{\tau^2 - 1}} \lesssim |\tan \pi z| \left[\frac{1}{\sqrt{\sigma^2 + a^2}} - \frac{1}{\sqrt{\sigma^2 + b^2}} \right].$$

(iii)

$$\int_1^{\frac{1}{\pi\sigma}} |I_{z2} + I_{z3}| \frac{d\tau}{\sqrt{\tau^2 - 1}} \lesssim \cos^2 \pi z \cos \pi z' [P_1(\sigma, z, z') + P_2(\sigma, z, z')].$$

Here,

$$P_1(\sigma, z, z') := \frac{2ab\pi}{4(b^2 - a^2)^3} \left[\frac{4}{\sqrt{\sigma^2 + b^2}} - \frac{4}{\sqrt{\sigma^2 + a^2}} + (b^2 - a^2) \left(\frac{1}{(\sigma^2 + a^2)^{3/2}} + \frac{1}{(\sigma^2 + b^2)^{3/2}} \right) \right],$$

$$P_2(\sigma, z, z') := \frac{\pi^3}{4(b^2 - a^2)^3} \left[\frac{4b^2}{\sqrt{\sigma^2 + b^2}} - \frac{4a^2}{\sqrt{\sigma^2 + a^2}} + (b^2 - a^2) \left(\frac{2\sigma^2 + a^2}{(\sigma^2 + a^2)^{3/2}} + \frac{2\sigma^2 + b^2}{(\sigma^2 + b^2)^{3/2}} \right) \right].$$

Proof of Proposition 5.2. Using the results from the above lemmas, a suitable function $H(\sigma, z, z')$ that works in (5.22) is

$$H(\sigma, z, z') := c \left(\frac{1}{\sigma} \left[\frac{1}{\sqrt{\sigma^2 + a^2}} - \frac{1}{\sqrt{\sigma^2 + b^2}} \right] + |\tan \pi z| \left[\frac{1}{\sqrt{\sigma^2 + a^2}} - \frac{1}{\sqrt{\sigma^2 + b^2}} \right] + \cos^2 \pi z \cos \pi z' [P_1(\sigma, z, z') + P_2(\sigma, z, z')] + \frac{\cos \pi z'}{\sigma} \right),$$

when $(\sigma, z, z') \in (0, 1/2\pi) \times (-1/2, 1/2) \times (-1/2, 1/2)$ and

$$H(\sigma, z, z') := c \cos \pi z' \exp(-\pi\sigma),$$

when $(\sigma, z, z') \in [1/2\pi, \infty) \times (-1/2, 1/2) \times (-1/2, 1/2)$. Here, $c > 0$ is some positive constant. With this definition of the function H and Lemma B.1 from appendix B, we can obtain a bound on the integral (5.23) as

$$\begin{aligned} \int_0^\infty \sigma H(\sigma, z, z') d\sigma &\lesssim \log \left(1 + \frac{4(b^2 - a^2)}{3a^2} \right) + \frac{\cos \pi z'}{b} + \frac{\cos^2 \pi z \cos \pi z'}{b^3} + \cos \pi z' \\ &\lesssim \log \left(1 + \frac{(b^2 - a^2)}{a^2} \right) + \frac{\cos \pi z'}{b}. \end{aligned} \quad (5.28)$$

Here, we used (5.13a) to obtain the last line. \square

Proof of Lemma 5.1. We first note that

$$\begin{aligned} \int_1^\infty (|I_{\sigma 1}| + |I_{\sigma 2}| + |I_{\sigma 3}|) \frac{d\tau}{\sqrt{\tau^2 - 1}} &\leq \int_1^2 (|I_{\sigma 1}| + |I_{\sigma 2}| + |I_{\sigma 3}|) \frac{d\tau}{\sqrt{\tau^2 - 1}} \\ &\quad + 2 \int_2^\infty (|I_{\sigma 1}| + |I_{\sigma 2}| + |I_{\sigma 3}|) \frac{d\tau}{\tau}. \end{aligned} \quad (5.29)$$

We also have

$$\begin{aligned} \int_1^\infty (|I_{z1}| + |I_{z2}| + |I_{z3}|) \frac{d\tau}{\sqrt{\tau^2 - 1}} &\leq \int_1^2 (|I_{z1}| + |I_{z2}| + |I_{z3}|) \frac{d\tau}{\sqrt{\tau^2 - 1}} \\ &\quad + \int_2^\infty (|I_{z1}| + |I_{z2}| + |I_{z3}|) d\tau. \end{aligned} \quad (5.30)$$

Now the assumption in the lemma is $\sigma \geq 1/2\pi$. So, if $\tau \geq 1$, then

$$\cosh(\pi\tau\sigma) - 1 \geq \frac{\cosh(\pi\tau\sigma)}{8},$$

and we always have

$$\sinh(\pi\tau\sigma) \leq \cosh(\pi\tau\sigma) \quad \text{and} \quad \frac{\exp(\pi\tau\sigma)}{2} \leq \cosh(\pi\tau\sigma).$$

Using these relations in (5.26a-f), one can show

$$\begin{aligned} |I_{\sigma 1}| &\lesssim \cos(\pi z') \tau \exp(-\pi\tau\sigma), & |I_{\sigma 2}| &\lesssim \cos(\pi z') \tau \exp(-\pi\tau\sigma), & |I_{\sigma 3}| &\lesssim \cos(\pi z') \tau \exp(-\pi\tau\sigma), \\ |I_{z 1}| &\lesssim \cos(\pi z') \exp(-\pi\tau\sigma), & |I_{z 2}| &\lesssim \cos(\pi z') \exp(-2\pi\tau\sigma), & |I_{z 3}| &\lesssim \cos(\pi z') \exp(-2\pi\tau\sigma). \end{aligned}$$

In total, we obtain

$$|I_{\sigma 1}| + |I_{\sigma 2}| + |I_{\sigma 3}| \lesssim \cos(\pi z') \tau \exp(-\pi\tau\sigma), \quad (5.31a)$$

$$|I_{z 1}| + |I_{z 2}| + |I_{z 3}| \lesssim \cos(\pi z') \exp(-\pi\tau\sigma). \quad (5.31b)$$

Next, we substitute (5.31a) in (5.29) and (5.31b) in (5.30). We also use the fact $\exp(-\pi\tau\sigma) \leq \exp(-\pi\sigma)$ for the integrals carried from $\tau = 1$ to $\tau = 2$ in (5.29) and (5.30), which leads to

$$\begin{aligned} \int_1^\infty (|I_{\sigma 1}| + |I_{\sigma 2}| + |I_{\sigma 3}|) \frac{d\tau}{\sqrt{\tau^2 - 1}} &\lesssim \cos(\pi z') \exp(-\pi\sigma) + \cos(\pi z') \frac{\exp(-2\pi\sigma)}{\pi\sigma} \\ &\lesssim \cos(\pi z') \exp(-\pi\sigma), \end{aligned} \quad (5.32)$$

and

$$\begin{aligned} \int_1^\infty (|I_{z 1}| + |I_{z 2}| + |I_{z 3}|) \frac{d\tau}{\sqrt{\tau^2 - 1}} &\lesssim \cos(\pi z') \exp(-\pi\sigma) + \cos(\pi z') \frac{\exp(-2\pi\sigma)}{\pi\sigma} \\ &\lesssim \cos(\pi z') \exp(-\pi\sigma). \end{aligned} \quad (5.33)$$

□

Proof of Lemma 5.2. The proof is similar to the proof of lemma 5.1. □

Proof of Lemma 5.3. First, we establish a few simple relations. The assumption in the lemma is $\sigma < \frac{1}{2\pi}$. So, if $1 \leq \tau \leq \frac{1}{\pi\sigma}$, then

$$\sinh(\pi\sigma\tau) \leq (\pi\sigma\tau) \sinh(1), \quad \cosh(\pi\sigma\tau) \leq \cosh(1), \quad \text{and} \quad \cosh(\pi\sigma\tau) \leq 1 + (\cosh(1) - 1)\pi^2\sigma^2\tau^2,$$

and we always have

$$\cosh(\pi\sigma\tau) \geq 1 + \frac{(\pi\sigma\tau)^2}{2}.$$

(i) We can then use the relations above to derive a simple bound on $|I_{\sigma 1}|$:

$$|I_{\sigma 1}| \leq I_{\sigma 1}^b := \frac{2 \cosh(1) \cos(\pi z) \cos(\pi z') \tau}{\pi^4 [\sigma^2 \tau^2 + a^2] [\sigma^2 \tau^2 + b^2]}.$$

We can also obtain a simple bound on $|I_{\sigma 2}|$ as follows

$$\begin{aligned} |I_{\sigma 2}| &\leq \frac{4 \sinh^2(1) \cos(\pi z) \cos(\pi z') \sigma^2 \tau^3}{\pi^4 [\sigma^2 \tau^2 + a^2]^2 [\sigma^2 \tau^2 + b^2]} \\ &\leq \frac{4 \sinh^2(1) \cos(\pi z) \cos(\pi z') \tau}{\pi^4 [\sigma^2 \tau^2 + a^2] [\sigma^2 \tau^2 + b^2]} = \frac{2 \sinh^2(1)}{\cosh(1)} I_{\sigma 1}^b. \end{aligned}$$

With a similar calculation, we prove that the same bound also holds for $|I_{\sigma 3}|$. We can now finish the proof as

given below

$$\int_1^{\frac{1}{\pi\sigma}} |I_{\sigma 1}| + |I_{\sigma 2}| + |I_{\sigma 3}| \frac{d\tau}{\sqrt{\tau^2 - 1}} \lesssim \int_1^\infty |I_{\sigma 1}^b| \frac{d\tau}{\sqrt{\tau^2 - 1}} \lesssim \frac{1}{\sigma} \left[\frac{1}{\sqrt{\sigma^2 + a^2}} - \frac{1}{\sqrt{\sigma^2 + b^2}} \right].$$

(ii) We can obtain a following simple bound on $|I_{z1}|$ as

$$|I_{z1}| \leq \frac{2\pi\sigma \sinh(1) |\sin \pi z| \cos \pi z' \tau}{\pi^4 [\sigma^2 \tau^2 + a^2] [\sigma^2 \tau^2 + b^2]} = (\pi\sigma) \tanh(1) |\tan(\pi z)| I_{\sigma 1}^b.$$

Performing an integration in τ as in part (i) leads to the desired result.

(iii) We first obtain a simple bound on the sum $I_{z2} + I_{z3}$ given as follows

$$\begin{aligned} I_{z2} + I_{z3} &= \frac{\cos^2(\pi z) \cos(\pi z') \sinh(\pi\tau\sigma) [\sin \pi z' \cosh(\pi\tau\sigma) - \sin \pi z]}{[\cosh(\pi\tau\sigma) + \cos \pi(z' + z)]^2 [\cosh(\pi\tau\sigma) - \cos \pi(z' - z)]^2}, \\ \Rightarrow |I_{z2} + I_{z3}| &\leq \frac{16}{\pi^7} \cos^2(\pi z) \cos(\pi z') \frac{\sigma\tau [|\sin \pi z' - \sin \pi z| + \pi^2 \sigma^2 \tau^2]}{[\sigma^2 \tau^2 + a^2]^2 [\sigma^2 \tau^2 + b^2]^2}. \end{aligned}$$

This result, combined with the following integrals

$$\begin{aligned} \int_1^\infty \frac{\sigma\tau}{[\sigma^2 \tau^2 + a^2]^2 [\sigma^2 \tau^2 + b^2]^2} \frac{d\tau}{\sqrt{\tau^2 - 1}} &= \\ \frac{\pi}{4(b^2 - a^2)^3} \left[\frac{4}{\sqrt{\sigma^2 + b^2}} - \frac{4}{\sqrt{\sigma^2 + a^2}} + (b^2 - a^2) \left(\frac{1}{(\sigma^2 + a^2)^{3/2}} + \frac{1}{(\sigma^2 + b^2)^{3/2}} \right) \right], \\ \int_1^\infty \frac{\sigma^3 \tau^3}{[\sigma^2 \tau^2 + a^2]^2 [\sigma^2 \tau^2 + b^2]^2} \frac{d\tau}{\sqrt{\tau^2 - 1}} &= \\ \frac{\pi}{4(b^2 - a^2)^3} \left[\frac{4b^2}{\sqrt{\sigma^2 + b^2}} - \frac{4a^2}{\sqrt{\sigma^2 + a^2}} + (b^2 - a^2) \left(\frac{2\sigma^2 + a^2}{(\sigma^2 + a^2)^{3/2}} + \frac{2\sigma^2 + b^2}{(\sigma^2 + b^2)^{3/2}} \right) \right], \end{aligned}$$

leads to the desired result. \square

6 Discussion

In this paper, we studied the problem of optimizing the heat transfer between two differentially heated parallel plates by incompressible flows that satisfy an enstrophy constraint ($\langle |\nabla \mathbf{u}|^2 \rangle \leq \mathcal{P}$) and no-slip boundary conditions. The main result of this paper was to show that the previously derived upper bound on the heat transfer are sharp in the scaling with \mathcal{P} , which we demonstrated by constructing an explicit example of three-dimensional branching pipe flows. In this section, we discuss the implications of our result in the context of (1) anomalous dissipation in a passive scalar and (2) Rayleigh–Bénard convection.

6.1 Anomalous dissipation in a passive scalar

The initial motivation for our study was a result by Drivas *et al.* ([DELJ22]), regarding the anomalous dissipation in a passive scalar transport. They constructed a velocity field $\mathbf{u} \in C^\infty([0, \tau] \times \mathbb{T}^d) \cap L^1([0, \tau]; C^\alpha(\mathbb{T}^d))$, where $d \geq 2$, τ is a fixed time and $\alpha < 1$, such that the solution of the advection-diffusion equation

$$\partial_t T^\kappa + \mathbf{u} \cdot \nabla T^\kappa = \kappa \Delta T^\kappa$$

follows

$$\liminf_{\kappa \rightarrow 0} \kappa \int_0^\tau \int_{\mathbb{T}^d} |\nabla T^\kappa|^2 d\mathbf{x} dt \geq \chi > 0,$$

where χ may depend on the initial data. While this result was obtained for a periodic domain, we were inspired by the possibility of proving such a result in a domain with boundaries. After appropriately rescaling the velocity fields that we created to prove Theorem 1.1, we can state a weak result in this direction.

Corollary 6.1. *For a constant $\kappa_0 > 0$, there exist velocity fields \mathbf{u}^κ , for every $0 < \kappa < \kappa_0$, such that $\|\mathbf{u}^\kappa\|_{H_0^1(\Omega)} \leq 1$ and the solution of the steady advection diffusion equation: $\mathbf{u}^\kappa \cdot \nabla T^\kappa = \kappa \Delta T^\kappa$ in Ω with boundary conditions $T^\kappa = 1$ at $z = -1/2$ and $T^\kappa = 0$ at $z = 1/2$ obeys*

$$\liminf_{\kappa \rightarrow 0} \kappa^{2/3} \int_{\Omega} |\nabla T^\kappa|^2 d\mathbf{x} \geq \chi_0 > 0. \quad (6.1)$$

for a constant χ_0 .

We see from (6.1) that the exponent for κ is $2/3$, which is less than one. Therefore this corollary is not as strong as the statement we would have hoped to prove. However, the a priori upper bound (1.9) also shows that this is the best result one can achieve in the setting considered in Corollary 6.1. However, if we allow the velocity field to be less smooth, in particular, we allow \mathbf{u}^κ to be only uniformly bounded in the L^2 norm, then we can indeed prove

$$\liminf_{\kappa \rightarrow 0} \kappa \int_{\Omega} |\nabla T^\kappa|^2 d\mathbf{x} \geq \chi_0 > 0. \quad (6.2)$$

This can be shown after appropriately rescaling the velocity fields of [DT19] used to prove Theorem 1.1 in their paper. Another possibility is to allow the walls to be rough. This has not yet, to our knowledge, been investigated, which raises the following question: if we allow the boundary of the domain, which locally is the graph of functions that are α -Hölder continuous with exponent $\alpha < 1$, can one also prove (6.2) in that case? Physically, it would mean that we are increasing the heat transfer by letting the area of walls go to infinity. Indeed, it is known in the literature that fractal boundaries tend to enhance heat transfer ([TWDW21]). Answer to such a question will, therefore, help in understanding the role played by rough boundaries in increasing the heat transfer. Along the same line, it would also be interesting to investigate the role played by a slip boundary condition for the velocity field (see [DNN22] and a recent review by [Nob21]).

6.2 Rayleigh–Bénard convection

Rayleigh–Bénard convection is the flow of fluid between two differentially heated parallel plates driven by buoyancy force. The flow is traditionally modeled by the Navier–Stokes equations under the Boussinesq approximation, written here in nondimensional form as

$$\partial_t \mathbf{u} + \mathbf{u} \cdot \nabla \mathbf{u} = -\nabla p + Pr \Delta \mathbf{u} + Pr Ra T \mathbf{e}_z, \quad (6.3a)$$

$$\partial_t T + \mathbf{u} \cdot \nabla T = \Delta T, \quad (6.3b)$$

where Ra is the Rayleigh number and Pr is the Prandtl number, respectively given by

$$Ra = \frac{g \alpha H^3 (T_B - T_T)}{\kappa \nu}, \quad Pr = \frac{\nu}{\kappa}.$$

In these above expressions, ν is the kinematic viscosity, κ is the thermal diffusivity, α is the coefficient of thermal expansion, H is the height of the domain, $T_B - T_T$ is the temperature difference and g is the magnitude of the gravitational acceleration acting in $-\mathbf{e}_z$ direction.

We solve the nondimensional governing equations (6.3a-b) in domain Ω with boundary conditions

$$\mathbf{u} = \mathbf{0}, \quad T = 1 \quad \text{at } z = -1/2 \quad \text{and} \quad \mathbf{u} = \mathbf{0}, \quad T = 0 \quad \text{at } z = 1/2.$$

The quantity of interest is the nondimensional heat transfer known as the Nusselt number Nu given by

$$Nu = 1 + \langle u_z T \rangle.$$

The angle brackets denote the long-time volume average and u_z is the component of the velocity in the z direction. Of course, Nu depends on the initial condition. However, Doering and Constantin ([DC96]) using the background method (see [FAW22] for a survey), proved the following a priori bound for any initial condition when $Ra \gg 1$:

$$Nu \lesssim Ra^{\frac{1}{2}}.$$

This bound is uniform in the Prandtl number Pr . To date, the best known upper bound, namely $Nu \leq 0.02634Ra^{\frac{1}{2}}$, was obtained by Plasting and Kerswell ([PK03]).

An important question is whether the scaling of this bound with respect to the Rayleigh number is sharp. Our result, in this context, proves that this scaling is indeed sharp if one replaces the momentum equation with a simple enstrophy condition.

$$\langle |\nabla \mathbf{u}|^2 \rangle = Ra(Nu - 1). \quad (6.4)$$

In other words Theorem 1.1 proves that, for large enough Rayleigh number, there exists velocity fields (depending on Ra) such that the solution of the advection-diffusion equation (6.3b) satisfies the relation (6.4) and for which

$$Nu \sim Ra^{\frac{1}{2}}.$$

APPENDIX

A Derivation of the variational principle for heat transfer (1.11)

In this appendix, we derive the variational principle given in (1.11). The proof is taken from the paper of Doering & Tobasco ([DT19]) and provided here for completeness. We begin by recalling

$$Q(\mathbf{u}) = \int_{\Omega} |\nabla T|^2 d\mathbf{x} = 1 + \int_{\Omega} u_z T d\mathbf{x}, \quad (A.1)$$

where T solves the steady convection diffusion equation and the velocity is assumed to be in $L^\infty(\Omega; \mathbb{R}^3)$. After substituting

$$T = \theta + \frac{1}{2} - z,$$

we obtain

$$Q(\mathbf{u}) = 1 + \int_{\Omega} |\nabla \theta|^2 d\mathbf{x} = 1 + \int_{\Omega} u_z \theta d\mathbf{x}, \quad (A.2)$$

where $\theta \in H_0^1(\Omega)$ solves

$$\mathbf{u} \cdot \nabla \theta = \Delta \theta + u_z \quad \text{in } \Omega,$$

and satisfies the homogeneous Dirichlet boundary conditions. Next, we consider a system of two PDEs.

$$\left. \begin{aligned} \mathbf{u} \cdot \nabla \eta_0 &= \Delta \xi_0 + u_z, \\ \mathbf{u} \cdot \nabla \xi_0 &= \Delta \eta_0, \end{aligned} \right\} \quad \text{in } \Omega, \quad (A.3a-b)$$

where both η_0 and ξ_0 satisfy the homogeneous Dirichlet boundary conditions. Clearly then

$$\theta = \eta_0 + \xi_0. \quad (A.4)$$

By multiplying the equation (A.3b) with ξ_0 and integrating, one obtains

$$\int_{\Omega} \nabla \eta_0 \cdot \nabla \xi_0 d\mathbf{x} = 0. \quad (A.5)$$

Next, we multiply the equation (A.3a) with η_0 and integrate and use (A.5) to obtain

$$\int_{\Omega} u_z \eta_0 \, d\mathbf{x} = 0. \quad (\text{A.6})$$

Finally, we substitute (A.4) in (A.2) and use (A.5) and (A.6) to get

$$Q(\mathbf{u}) - 1 = \int_{\Omega} |\nabla \xi_0|^2 + |\nabla \eta_0|^2 \, d\mathbf{x} = \int_{\Omega} u_z \xi_0 \, d\mathbf{x}, \quad (\text{A.7})$$

which after using (A.3b) can be rewritten as

$$Q(\mathbf{u}) - 1 = 2 \int_{\Omega} u_z \xi_0 \, d\mathbf{x} - \int_{\Omega} |\nabla \xi_0|^2 \, d\mathbf{x} - \int_{\Omega} |\nabla \Delta^{-1} \mathbf{u} \cdot \nabla \xi_0|^2 \, d\mathbf{x}, \quad (\text{A.8})$$

where Δ^{-1} denotes the inverse Laplacian operator in Ω corresponding to the homogeneous Dirichlet boundary conditions. We now consider the following maximization problem

$$\sup_{\xi \in H_0^1(\Omega)} 2 \int_{\Omega} u_z \xi \, d\mathbf{x} - \int_{\Omega} |\nabla \xi|^2 \, d\mathbf{x} - \int_{\Omega} |\nabla \Delta^{-1} \mathbf{u} \cdot \nabla \xi|^2 \, d\mathbf{x}, \quad (\text{A.9})$$

which is strictly concave, therefore, the only maximizer satisfies the Euler–Lagrange equation

$$\mathbf{u} \cdot \nabla \Delta^{-1} (\mathbf{u} \cdot \nabla \xi) = \Delta \xi + u_z.$$

We see that ξ_0 is the solution of above equation, therefore, ξ_0 maximizes (A.9), which then combined with (A.8) gives us

$$Q(\mathbf{u}) - 1 = \max_{\xi \in H_0^1(\Omega)} 2 \int_{\Omega} u_z \xi \, d\mathbf{x} - \int_{\Omega} |\nabla \xi|^2 \, d\mathbf{x} - \int_{\Omega} |\nabla \Delta^{-1} \mathbf{u} \cdot \nabla \xi|^2 \, d\mathbf{x}. \quad (\text{A.10})$$

To make this formulation homogeneous in the variable ξ , we consider the transformation $\xi \rightarrow s\xi$ and optimize in the scaling s to obtain

$$Q(\mathbf{u}) - 1 = \sup_{\substack{\xi \in H_0^1(\Omega) \\ \xi \neq 0}} \frac{(\int_{\Omega} u_z \xi \, d\mathbf{x})^2}{\int_{\Omega} |\nabla \xi|^2 \, d\mathbf{x} + \int_{\Omega} |\nabla \Delta^{-1} \text{div}(\mathbf{u} \xi)|^2 \, d\mathbf{x}}. \quad (\text{A.11})$$

Next, from the definition of $Q_{\max}^s(\mathcal{P})$ given in (1.5), we simply obtain

$$Q_{\max}^s(\mathbf{u}) - 1 = \sup_{\substack{\mathbf{u} \in L^\infty(\Omega) \\ \nabla \cdot \mathbf{u} = 0, \mathbf{u}|_{\partial\Omega} = \mathbf{0} \\ \int_{\Omega} |\nabla \mathbf{u}|^2 \, d\mathbf{x} \leq \mathcal{P}}} \sup_{\substack{\xi \in H_0^1(\Omega) \\ \xi \neq 0}} \frac{(\int_{\Omega} u_z \xi \, d\mathbf{x})^2}{\int_{\Omega} |\nabla \xi|^2 \, d\mathbf{x} + \int_{\Omega} |\nabla \Delta^{-1} \text{div}(\mathbf{u} \xi)|^2 \, d\mathbf{x}}. \quad (\text{A.12})$$

Finally, considering the following transformation

$$\mathbf{u} \rightarrow \frac{\mathcal{P}^{\frac{1}{2}}}{\int_{\Omega} |\nabla \mathbf{u}|^2 \, d\mathbf{x}} \mathbf{u}, \quad \xi \rightarrow \frac{\int_{\Omega} |\nabla \mathbf{u}|^2 \, d\mathbf{x}}{\mathcal{P}^{\frac{1}{2}}} \xi, \quad (\text{A.13})$$

in (A.12) leads to the desired result stated in Proposition 1.11.

B Bounds on a few integrals

Lemma B.1. *Let a and b be as given in (5.8). Let $z, z' \in (-1/2, 1/2)$ and $z \neq z'$, then the following estimates hold*

(i)

$$\int_0^1 \left[\frac{1}{\sqrt{\sigma^2 + a^2}} - \frac{1}{\sqrt{\sigma^2 + b^2}} \right] d\sigma \leq \frac{1}{2} \log \left(1 + \frac{4(b^2 - a^2)}{3a^2} \right). \quad (\text{B.1})$$

(ii)

$$\int_0^1 \left[\frac{\sigma}{\sqrt{\sigma^2 + a^2}} - \frac{\sigma}{\sqrt{\sigma^2 + b^2}} \right] d\sigma \leq \frac{b^2 - a^2}{b}. \quad (\text{B.2})$$

(iii)

$$\int_0^1 \sigma P_1(\sigma, z, z') d\sigma \leq \frac{\pi}{2b^3}. \quad (\text{B.3})$$

(iv)

$$\int_0^1 \sigma P_2(\sigma, z, z') d\sigma \leq \frac{\pi^3}{4b^3}. \quad (\text{B.4})$$

Proof of Lemma B.1.

Recall from the definition (5.8) of a and b that $a \leq b$, a fact which we will use in the proofs below.

(i)

$$\begin{aligned} \int_0^1 \left[\frac{1}{\sqrt{\sigma^2 + a^2}} - \frac{1}{\sqrt{\sigma^2 + b^2}} \right] d\sigma &= \frac{1}{2} \log \frac{1 + \sqrt{1 + a^2}}{1 + \sqrt{1 + b^2}} + \frac{1}{2} \log \frac{\sqrt{1 + b^2} - 1}{\sqrt{1 + a^2} - 1} \\ &\leq \frac{1}{2} \log \left(1 + \frac{\sqrt{1 + b^2} - \sqrt{1 + a^2}}{\sqrt{1 + a^2} - 1} \right) \\ &\leq \frac{1}{2} \log \left(1 + \frac{8(b^2 - a^2)}{3a^2 [\sqrt{1 + b^2} + \sqrt{1 + a^2}]} \right) \\ &\leq \frac{1}{2} \log \left(1 + \frac{4(b^2 - a^2)}{3a^2} \right). \end{aligned} \quad (\text{B.5})$$

(ii)

$$\int_0^1 \left[\frac{\sigma}{\sqrt{\sigma^2 + a^2}} - \frac{\sigma}{\sqrt{\sigma^2 + b^2}} \right] d\sigma = \sqrt{1 + a^2} - \sqrt{1 + b^2} + b - a \leq \frac{b^2 - a^2}{b + a} \leq \frac{b^2 - a^2}{b}. \quad (\text{B.6})$$

(iii)

$$\int_0^1 \sigma P_1(\sigma, z, z') d\sigma = \frac{\pi ab}{2} \left[\frac{1}{ab(b + a)^3} - \frac{1}{\sqrt{1 + a^2} \sqrt{1 + b^2} (\sqrt{1 + b^2} + \sqrt{1 + a^2})^3} \right] \leq \frac{\pi}{2b^3}. \quad (\text{B.7})$$

(iv)

$$\int_0^1 \sigma P_2(\sigma, z, z') d\sigma = \frac{\pi^3}{4} \left[\frac{1}{(b+a)^3} - \frac{1}{(\sqrt{1+b^2} + \sqrt{1+a^2})^3} - \frac{1}{\sqrt{1+a^2}\sqrt{1+b^2}(\sqrt{1+b^2} + \sqrt{1+a^2})^3} \right] \leq \frac{\pi^3}{4b^3}. \quad (\text{B.8})$$

□

C A few basic lemmas

Lemma C.1. Let $f \in C^0(\mathbb{R})$ such that $f'(r)$ exists for all $r \neq 0$. Now assume that $f'(r) \rightarrow f'_0$ as $r \rightarrow 0$ for some finite f'_0 , then $f'(0)$ exists and its value is f'_0 .

Proof of Lemma C.1. Using the mean value theorem, we have

$$\frac{f(h) - f(0)}{h} = f'(\eta) \quad \text{for some } \eta \in (0, h), \quad (\text{C.1})$$

The proof of lemma follows by taking $h \rightarrow 0$. □

Definition C.1. A function $f : \mathbb{R} \rightarrow \mathbb{R}$ is said to have the property (N) if

$$f \in C^\infty(\mathbb{R}) \quad \text{and} \quad \left. \frac{d^{2n-1}f(r)}{dr^{2n-1}} \right|_{r=0} = 0 \quad \forall n \in \mathbb{N}. \quad (\text{C.2})$$

It is clear that if $f(r)$ has the property (N) then so does the $f(\alpha r)$ for any $\alpha \neq 0$. Furthermore, we have the following lemma.

Lemma C.2. If a function $f : \mathbb{R} \rightarrow \mathbb{R}$ has the property (N) then so does the function $g : \mathbb{R} \rightarrow \mathbb{R}$ defined as

$$g(r) := \begin{cases} \frac{1}{r} \frac{df(r)}{dr} & \text{if } r \neq 0, \\ f''(0) & \text{if } r = 0, \end{cases} \quad (\text{C.3})$$

has the property (N).

Proof of Lemma C.2. It is clear that $g(r)$ is continuous when $r \neq 0$. Now from L'Hospital's rule we obtain

$$\lim_{r \rightarrow 0} \frac{1}{r} \frac{df(r)}{dr} = \lim_{r \rightarrow 0} \frac{d^2f(r)}{dr^2} = f''(0), \quad (\text{C.4})$$

therefore, using Lemma C.1, $g(r)$ is continuous at $r = 0$ as well. Now, for $n \geq 1$, we have

$$\frac{d^n g(r)}{dr^n} = \frac{n!}{r^{n+1}} \sum_{i=0}^n \frac{(-1)^{n-i} r^i}{i!} \frac{d^{i+1} f(r)}{dr^{i+1}} \quad \text{if } r \neq 0. \quad (\text{C.5})$$

Taking the limit $r \rightarrow 0$ and using the L'Hospital's rule, we obtain

$$\begin{aligned} \lim_{r \rightarrow 0} \frac{d^n g(r)}{dr^n} &= \lim_{r \rightarrow 0} \frac{n!}{r^{n+1}} \sum_{i=0}^n \frac{(-1)^{n-i} r^i}{i!} \frac{d^{i+1} f(r)}{dr^{i+1}} \\ &= \lim_{r \rightarrow 0} \frac{n!}{(n+1)r^n} \left[\sum_{i=0}^n \frac{(-1)^{n-i} r^i}{i!} \frac{d^{i+2} f(r)}{dr^{i+2}} - \sum_{i=1}^n \frac{(-1)^{n-i-1} r^{i-1}}{(i-1)!} \frac{d^{i+1} f(r)}{dr^{i+1}} \right] \\ &= \frac{1}{(n+1)} \left. \frac{d^{n+2} f(r)}{dr^{n+2}} \right|_{r=0}. \end{aligned} \quad (\text{C.6})$$

Noting that g is continuous and using Lemma C.1 and the formula (C.6), for $n = 1$, we see that $g(r)$ is differentiable at $r = 0$, furthermore, $g'(r)$ is continuous everywhere. Proceeding in a similar manner, an induction argument then shows that g is infinitely differentiable. Once again, noting from the formula (C.6) that all the odd derivatives of g are zero at $r = 0$, proves the lemma. \square

Lemma C.3. *Let $g : \mathbb{R}^2 \rightarrow \mathbb{R}$ be given by $g(y, z) = y^{\alpha_y} z^{\alpha_z} f(\varrho)$, where α_y and α_z are nonnegative integers and ϱ is a placeholder for $\sqrt{y^2 + z^2}$. Furthermore, the function $f : \mathbb{R} \rightarrow \mathbb{R}$ has the property (N). Then the function g is infinitely differentiable.*

Proof. We can prove this lemma using an induction argument combined with Lemma C.2. \square

Now it is a standard exercise in classical real analysis to show that the functions $\bar{\varphi}(r)$, $h(r)$, $\Psi_s(r)$, $\Psi_e(r)$, $\frac{\Psi_s(r)}{r^2}$ and $\frac{\Psi_e(r)}{r^2}$, with relevant definitions given in (4.10), (4.16) and (4.18), have the property (N). Using Lemma C.3, one can then conclude that the velocity field, as defined in (4.18), is infinitely smooth.

References

- [AK18] T. Alam and M.-H. Kim. A comprehensive review on single phase heat transfer enhancement techniques in heat exchanger applications. *Renewable and Sustainable Energy Reviews*, 81:813–839, 2018. doi:[10.1016/j.rser.2017.08.060](https://doi.org/10.1016/j.rser.2017.08.060).
- [AM91] M. Avellaneda and A. J. Majda. An integral representation and bounds on the effective diffusivity in passive advection by laminar and turbulent flows. *Comm. Math. Phys.*, 138(2):339–391, 1991. URL <http://projecteuclid.org/euclid.cmp/1104202948>.
- [Aro00] C. P. Arora. *Refrigeration and air conditioning*. Tata McGraw-Hill Education, 2000.
- [Bus69] F. H. Busse. On howard’s upper bound for heat transport by turbulent convection. *Journal of Fluid Mechanics*, 37(3):457–477, 1969. doi:[10.1017/S0022112069000668](https://doi.org/10.1017/S0022112069000668).
- [DC96] C. R. Doering and P. Constantin. Variational bounds on energy dissipation in incompressible flows. iii. convection. *Physical Review E*, 53(6):5957, 1996. doi:[10.1103/PhysRevE.53.5957](https://doi.org/10.1103/PhysRevE.53.5957).
- [DC98] C. R. Doering and P. Constantin. Bounds for heat transport in a porous layer. *J. Fluid Mech.*, 376:263–296, 1998. doi:[10.1017/S002211209800281X](https://doi.org/10.1017/S002211209800281X).
- [DEIJ22] T. D. Drivas, T. M. Elgindi, G. Iyer, and I.-J. Jeong. Anomalous dissipation in passive scalar transport. *Arch. Ration. Mech. Anal.*, 243(3):1151–1180, 2022. doi:[10.1007/s00205-021-01736-2](https://doi.org/10.1007/s00205-021-01736-2).
- [DNN22] T. D. Drivas, H. Q. Nguyen, and C. Nobili. Bounds on heat flux for rayleigh–bénard convection between navier-slip fixed-temperature boundaries. *Philosophical Transactions of the Royal Society A*, 380(2225):20210025, 2022. doi:[10.1098/rsta.2021.0025](https://doi.org/10.1098/rsta.2021.0025).
- [DT19] C. R. Doering and I. Tobasco. On the optimal design of wall-to-wall heat transport. *Comm. Pure Appl. Math.*, 72(11):2385–2448, 2019. doi:[10.1002/cpa.21832](https://doi.org/10.1002/cpa.21832).
- [FAW22] G. Fantuzzi, A. Arslan, and A. Wynn. The background method: Theory and computations. *Philosophical Transactions of the Royal Society A*, 380(2225):20210038, 2022. doi:[10.1098/rsta.2021.0038](https://doi.org/10.1098/rsta.2021.0038).
- [FP94] A. Fannjiang and G. Papanicolaou. Convection enhanced diffusion for periodic flows. *SIAM J. Appl. Math.*, 54(2):333–408, 1994. doi:[10.1137/S0036139992236785](https://doi.org/10.1137/S0036139992236785).
- [GMS98] M. Giaquinta, G. Modica, and J. Souček. *Cartesian currents in the calculus of variations. I*, volume 37 of *Ergebnisse der Mathematik und ihrer Grenzgebiete. 3. Folge. A Series of Modern Surveys in Mathematics [Results in Mathematics and Related Areas. 3rd Series. A Series of Modern Surveys in Mathematics]*. Springer-Verlag, Berlin, 1998. doi:[10.1007/978-3-662-06218-0](https://doi.org/10.1007/978-3-662-06218-0). Cartesian currents.

- [HCD14] P. Hassanzadeh, G. P. Chini, and C. R. Doering. Wall to wall optimal transport. *J. Fluid. Mech.*, 751:627–662, 2014. doi:[10.1017/jfm.2014.306](https://doi.org/10.1017/jfm.2014.306).
- [How63] L. N. Howard. Heat transport by turbulent convection. *J. Fluid Mech.*, 17:405–432, 1963. doi:[10.1017/S0022112063001427](https://doi.org/10.1017/S0022112063001427).
- [IV22] G. Iyer and T.-S. Van. Bounds on the heat transfer rate via passive advection. *SIAM J. Math. Anal.*, 54(2):1927–1965, 2022. doi:[10.1137/21M1394497](https://doi.org/10.1137/21M1394497).
- [Jak08] H. A. Jakobsen. *Chemical reactor modeling*. Springer, 2008. doi:[10.1007/978-3-319-05092-8](https://doi.org/10.1007/978-3-319-05092-8).
- [Mag12] F. Maggi. *Sets of finite perimeter and geometric variational problems*, volume 135 of *Cambridge Studies in Advanced Mathematics*. Cambridge University Press, Cambridge, 2012. doi:[10.1017/CBO9781139108133](https://doi.org/10.1017/CBO9781139108133). An introduction to geometric measure theory.
- [MDTY18] F. Marcotte, C. R. Doering, J.-L. Thiffeault, and W. R. Young. Optimal heat transfer and optimal exit times. *SIAM J. Appl. Math.*, 78(1):591–608, 2018. doi:[10.1137/17M1150220](https://doi.org/10.1137/17M1150220).
- [MKS18] S. Motoki, G. Kawahara, and M. Shimizu. Maximal heat transfer between two parallel plates. *J. Fluid Mech.*, 851:R4, 14, 2018. doi:[10.1017/jfm.2018.557](https://doi.org/10.1017/jfm.2018.557).
- [Nob21] C. Nobili. The role of boundary conditions in scaling laws for turbulent heat transport. *arXiv preprint arXiv:2112.15564*, 2021.
- [PK03] S. C. Plasting and R. R. Kerswell. Improved upper bound on the energy dissipation rate in plane Couette flow: the full solution to Busse’s problem and the Constantin-Doering-Hopf problem with one-dimensional background field. *J. Fluid Mech.*, 477:363–379, 2003. doi:[10.1017/S0022112002003361](https://doi.org/10.1017/S0022112002003361).
- [Sei15] C. Seis. Scaling bounds on dissipation in turbulent flows. *J. Fluid Mech.*, 777:591–603, 2015. doi:[10.1017/jfm.2015.384](https://doi.org/10.1017/jfm.2015.384).
- [STD20] A. N. Souza, I. Tobasco, and C. R. Doering. Wall-to-wall optimal transport in two dimensions. *J. Fluid. Mech.*, 889, 2020. doi:[10.1017/jfm.2020.42](https://doi.org/10.1017/jfm.2020.42).
- [TD17] I. Tobasco and C. R. Doering. Optimal wall-to-wall transport by incompressible flows. *Phys. Rev. Lett.*, 118(26):264502, 2017. doi:[10.1103/PhysRevLett.118.264502](https://doi.org/10.1103/PhysRevLett.118.264502).
- [Thu13] K. Thulukkanam. *Heat Exchanger Design Handbook, Second Edition*. Mechanical Engineering. Taylor & Francis, 2013.
- [Tob21] I. Tobasco. Optimal cooling of an internally heated disc. *arXiv preprint arXiv:2110.13291*, 2021.
- [TWDW21] S. Toppaladoddi, A. J. Wells, C. R. Doering, and J. S. Wettlaufer. Thermal convection over fractal surfaces. *J. Fluid Mech.*, 907:Paper No. A12, 26, 2021. doi:[10.1017/jfm.2020.826](https://doi.org/10.1017/jfm.2020.826).
- [WCKD15] B. Wen, G. P. Chini, R. R. Kerswell, and C. R. Doering. Time-stepping approach for solving upper-bound problems: Application to two-dimensional rayleigh-bénard convection. *Phys. Rev. E*, 92:043012, Oct 2015. doi:[10.1103/PhysRevE.92.043012](https://doi.org/10.1103/PhysRevE.92.043012).
- [WD11] J. P. Whitehead and C. R. Doering. Ultimate state of two-dimensional rayleigh-bénard convection between free-slip fixed-temperature boundaries. *Phys. Rev. Lett.*, 106:244501, Jun 2011. doi:[10.1103/PhysRevLett.106.244501](https://doi.org/10.1103/PhysRevLett.106.244501).